Defect types.

FAISAL, N., CORA, Ö.N., BEKCI, M.L., ŚLIWA, R.E., STERNBERG, Y., PANT, S., DEGENHARDT, R. and PRATHURU, A.

2021

Chapter 3
Defect Types

Nadimul Faisal, Ömer Necati Cora, Muhammed Latif Bekci, Romana Ewa Śliwa, Yehuda Sternberg, Shashank Pant, Richard Degenhardt, and Anil Prathuru

Abstract This chapter provides an overview of the common types of defects found in various structural materials and joints in aircraft. Materials manufacturing methods (including large-scale production) have been established in the aircraft industry. However, as will be seen in this chapter, manufacturing defects and defects during in-service conditions are very common across all material types. The structural material types include metals, composites, coatings, adhesively bonded and stir-welded joints. This chapter describes the defect types as a baseline for the description of their detection with the methods of Chap. 5 to 8. Based on the understanding of the defect types, there is great expectation for a technical breakthrough for the application of structural health monitoring (SHM) damage detection systems, where continuous monitoring and assessment with high throughput and yield will produce the desired structural integrity.

N. Faisal (✉) · A. Prathuru
Robert Gordon University, Aberdeen, UK
e-mail: n.h.faisal@rgu.ac.uk

Ö. N. Cora · M. L. Bekci
Karadeniz Technical University, Trabzon, Turkey

R. E. Śliwa
Rzeszow University of Technology, Rzeszow, Poland

Y. Sternberg
Israel Aerospace Industries Ltd, Ben Gurion, Israel

S. Pant
National Research Council Canada, Ottawa, ON, Canada

R. Degenhardt
German Aerospace Center (DLR), Braunschweig, Germany

3.1 Metallic Materials

Load bearing aircraft structure is assembled and built using several major components such as fuselage, wings, engines and landing gear, as shown in Fig. 3.1. Among material types, metallic materials used in the aircraft structure manufacturing and assembly include aluminium, high-strength steel, titanium and superalloys (nickel, iron–nickel and cobalt-based alloys) with each possessing certain qualities that make them ideal for this use. Aluminium alloys have been the main airframe material. The attractiveness of aluminium alloys is that it is relatively low cost, lightweight, easily heat-treated to high strength levels and most easily fabricated with low costs. Titanium alloys can often be used to save weight by replacing heavier steel alloys in the airframe and superalloys in the low-temperature parts of gas turbines, and they are used instead of aluminium alloys when the temperature requirements exceed aluminium capabilities or when fatigue or corrosion has been a recurring problem. High-strength steels (HSS) are used for highly critical parts such as landing gear components. The main advantages of HSS are their high strengths and stiffness, but they are of high density and susceptible to brittle fracture. Superalloys are used extensively in jet turbine engines, when the temperature of exploitation excess 80% of the incipient melting temperatures while exhibiting high strength, good fatigue, creep resistance, good corrosion resistance and ability to work at high temperatures.
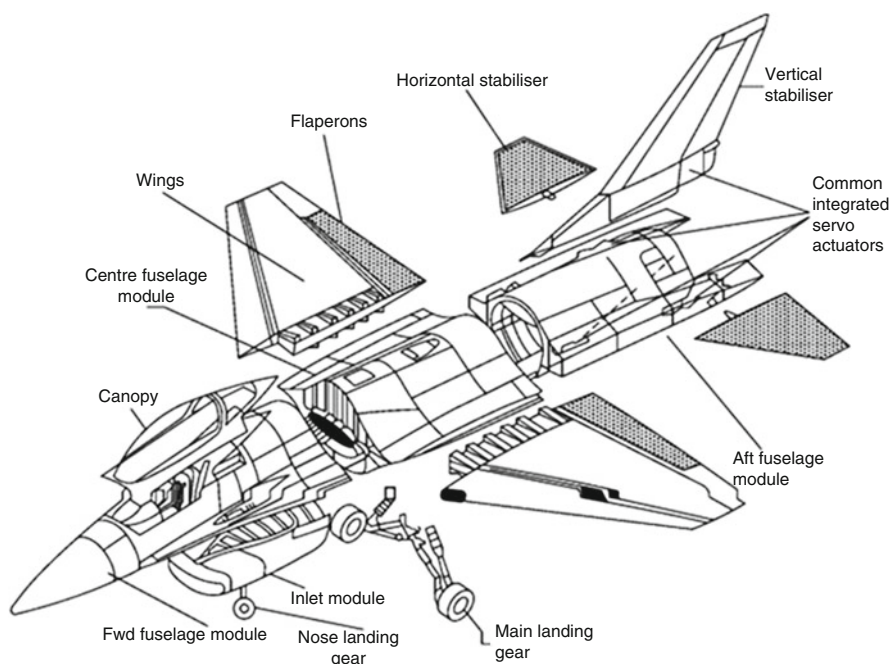
Fig. 3.1 Main structural components of a modern military aircraft (Mouritz 2012a, 2012b, 2012c)

Both magnesium and beryllium alloys as extremely lightweight materials (competitive on specific strength and specific modulus) are considered for applications. In the case of magnesium alloys, the biggest obstacle to use them is their extremely poor corrosion resistance; hence, the products require special solutions for protection. Beryllium alloys represent an attractive combination of properties, but they must be processed using powder metallurgy technology with the requirement for controlled manufacturing environments and the concern for safety during the repair/service of deployed structures (Śliwa et al. 2016; Peel and Gregson 1995; Campbell 2006; Śliwa et al. 2017).

Note that safety-critical aircraft structure demands metallic materials that are both durable and lightweight, as well as being able to withstand severe structural stress at various altitudes and temperatures, including fatigue and wear resistance. High-quality material requirements for aeronautical applications make the defect detection and inspection techniques of prime importance, both in manufacturing and in-service operation. The following subsections describe the major defects encountered in metallic materials.

3.1.1 Defects During the Manufacturing Process

Metallic materials or their alloys are a class of elementary materials, such as aluminium, steel, titanium and nickel alloys, all of which are crystalline when solid. Given pure metals, some of the important defect types can be point defect, line defect and plane defect (Gilbert 2020). A point defect involves only a single particle (called a lattice point). A line defect is limited to a row of lattice points. A plane defect involves an entire plane of lattice points in a crystal. A vacancy occurs where an atom is missing from the crystalline array, constituting a tiny void in the middle of a solid.

There are four fundamental mechanisms for introducing a point defect into the structure of a solid (Hiroshi 2014; Fang 2018), such as (a) when a particle is missing at one or more lattice sites, a vacancy is attained; (b) when a particle forces its way into a hole between lattice sites, interstitial impurity is attained; (c) substitutional impurities result from replacing the particle that should occupy a lattice site with a different particle and (d) dislocations are unidirectional defects caused by holes that are not large enough to be a vacancy.

When a fraction of the original materials are replaced by impurities, a solid solution can be attained. Alloys are examples of solid solutions. Lattice distortions of the crystalline materials often occur when impurities are added to a solid. Thus, point defects often determine the properties of a material. Point defects can change the mechanical properties, such as strength, malleability or ductility. Dissolving a small percentage of carbon in pure iron (i.e. making it a steel) makes it stronger than iron; however, higher percentages of carbon can make the steel harder and more brittle.

A dislocation mechanism (screw or edge dislocation types) can weaken a metal, as it allows planes of atoms in a solid to move one row at a time. Interestingly, they can also strengthen a metal when work hardened during heating, hammering, cooling, reheating and reworking. In the course of the work hardening process, intersecting dislocations (i.e. when planes of atoms move one row at a time) that impede the movement of planes of atoms are created.

Most metallic materials are polycrystalline in nature (i.e. structure with many crystallites of varying size and orientation), whereas a group of crystals is called grains. Crystal grains in polycrystalline metallic materials deform by slips on specific slip systems. The place where two grains meet is called a grain boundary. The movement of a deformation through a solid polycrystalline tends to stop at a grain boundary. Therefore, managing the grain size in solids is necessary to obtain a desirable mechanical property, and fine-grained polycrystalline materials are usually stronger than coarse-grained ones.

3.1.2 Defects During In-service Conditions

From early aircraft to the most advanced ones, different types of materials are used in the aerospace industry. Metals have been the most preferred materials and served as the primary choice of materials for many years because of its versatile features and properties. Although the use of advanced composites is continuously increasing in aircraft, metallic materials still constitute 45% of the total weight (20% aluminium, 15% titanium and 10% steel) of the Boeing 787 aircraft. Aluminium is exploited in wings and tail leading edges; titanium is primarily exploited on engine parts and fasteners while steel is used in several places including landing gears, leading edge of the wings, engine pylons, hinges, cables, fasteners, etc.. Airbus A350 has a similar material distribution, 20% Al, Al–Li alloys, 14% titanium and 7% steel by weight (Criou 2007).

Defects and its prevention in aerospace materials are uttermost concerns since undetectable flaws can cause catastrophic consequences for aircraft and passengers. The defects can be categorized, from the origin point of view, under four headings: (a) due to manufacturing, (b) during assembly, (c) during transport and (d) during service. This subsection is intended to shed light on the in-service related defects of aerospace materials. Defects during in-service mainly occur because of either inadequate material specification; in other words, inappropriate material choice and operation beyond the intended design parameters (Archer and McIlhagger 2015).

The common characteristic of in-service damage is that they occur unexpectedly, and it might be difficult to predict and diagnose it. Table 3.1 shows the most common causes of failure. The following subsections describe the major defects or failure types encountered in metallic structures.

Table 3.1 Percentage of the failures in aircraft components (Brooks and Choudhury 2002; Findlay and Harrison 2002)

Failure type	Percentage (%) of failures
Fatigue	55–61
Corrosion	3–16
Overload	14–18
Stress-corrosion-cracking/corrosion fatigue/hydrogen embrittlement	7–8
Wear	6–7
High-temperature corrosion	2
Creep	1

**Table 3.2** Fatigue causes for some aircraft accidents (Tiffany et al. 2010)

Fatigue causes	Numbers of accidents	
	Airframes	Engine discs
Unanticipated high local stresses	11	-
Manufacturing defect or tool mark	3	2
Material defect	2	1
Maintenance deficiencies	6	-
Abnormally high fan speed	-	1

3.1.2.1 Fatigue

Fatigue is the primary reason for failure in aerospace metals that occurs under repeated loads leading to premature failure of structural parts. If it is not detected in the early stages, it can cause catastrophic failures. It is usually characterized as the initiation and propagation of cracks to an unaccepted size. Fatigue is mostly controlled with stress history, material properties, chemical environment and manufacturing quality (Arrieta and Striz 2005). Table 3.2 shows a summary of the common fatigue causes observed in aircraft that have led to accidents, whereas Fig. 3.2 shows the structural areas prone to fatigue damage in early Airbus A300 design.

The frequency, sign, sequence and magnitude of repeated loads affect the fatigue rate, its initiation and growth. Besides these, corrosive environment, loading rate and temperature may play role in fatigue. Several early aircraft accidents were related with stress concentration that initiated cracks under operational loads. These stress concentrations were not detected until the accidents occurred. Stress concentration was not the only reason for early aircraft accidents, but several other factors including the use of high strength material with low fatigue crack resistance and tolerance (very short final crack size) and manufacturing process, material-oriented defects are involved. In August 29, 1948, Martin 202-type aircraft belonging to Northwest Airlines crashed near in Winona, Minnesota, during a Chicago–Minneapolis scheduled flight killing all 37 persons aboard. The accident caused by
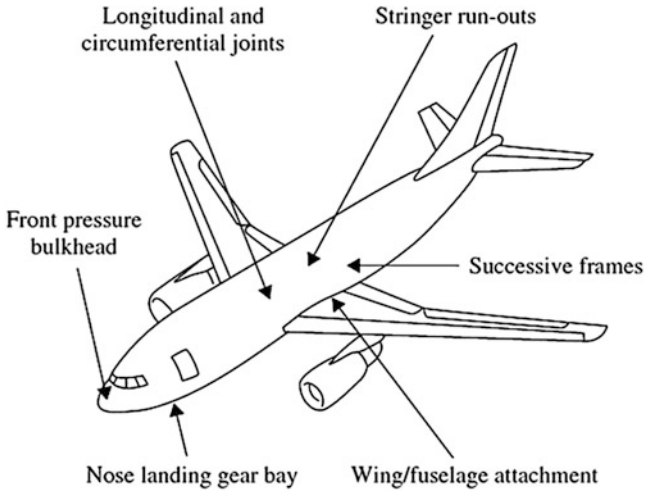
Fig. 3.2 Common fatigue failure zones for Airbus A300 (Brand and Boller 1999)

the left-wing separation from the aircraft during thunderstorm related turbulence conditions. Investigations conducted by Civil Aeronautics Board revealed that a fatigue crack caused the detachment of outer wing (made of AA 7075-T6 alloy) from the rest of the wing. The aircraft design was not based on fail-safe approach at that time and this accident along with other Comet type aircraft failures led to the development of "Fail-Safe Design" approach (Tiffany et al. 2010; Ruth 1973). This approach is regarded as the extension of the safe-life concept in which the component or system is designed in a way thay it will not fail within a specified period. After this period, the part is removed from the service. In Fail-Safe approach, however; in case of specific type of failure, the component or system should carry an honourable service load even after one of its components fail. In this approach, different from Safe-Life, the failure for specific part is possible, yet the system design prevents or at least mitigates the unsafe consequences of the system's catastrophic failure. In other words, the part may fail yet it does not trigger the failure of other parts and, it remains as safe as it was before the failure (Mills et al. 2009; McBrearty 1956). Figure 3.3 shows the schematic for the wing root assembly failure for a Martin 202 aircraft.

More recently, Rebhi et al. examined the reason for the fracturing of the ADF antenna placed just behind the cockpit of a military aircraft (Rebhi et al. 2018). Figure 3.4a shows the ADF antenna location on the aircraft while Fig. 3.4b shows where it breaks. Note that the upper portion of the antenna was fractured because of the fatigue initiated by the corrosion pits. The crack origin was found to be at the outer surface on the antenna by tracing back the beach mark Fig. 3.5.
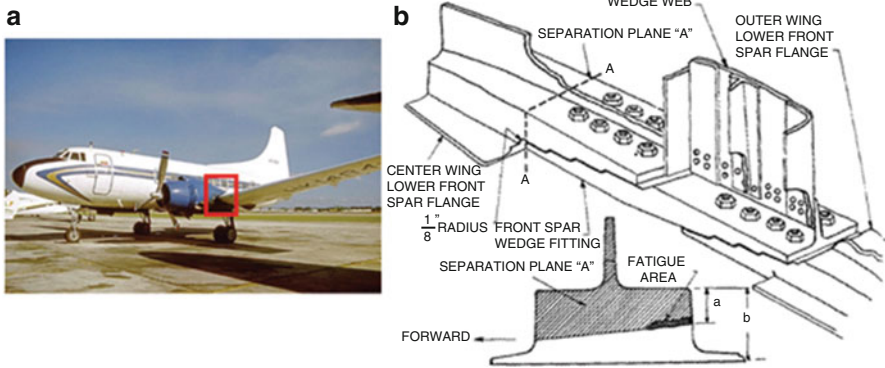
Fig. 3.3 (**a**) A typical Martin 202 aircraft (produced by Glenn L. Martin Company during 1947–1948) with approximate fatigue location (in red box) (Ruth 1973), (**b**) schematic section of separation of lower flange showing fatigue are and also sudden increase of depth of flange 'a' to approximately twice the depth as indicated by 'b' (after Civil Aeronautics Board 1949)
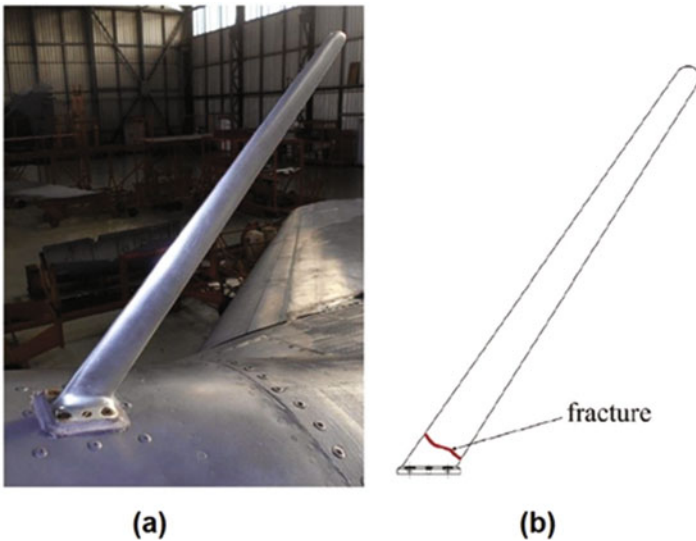
Fig. 3.4 Fractured ADF antenna of a military aircraft (**a**) location of antenna, (**b**) breaking line (Rebhi et al. 2018)

3.1.2.2 Corrosion

Any metallic part in an aircraft is prone to corrosion. Corrosion, generally, can be defined as deterioration of metals by electrochemical reaction with surrounding environment and gradual material loss. It is one of the serious concerns especially for older aircraft and responsible for 25% of the metallic component failures.
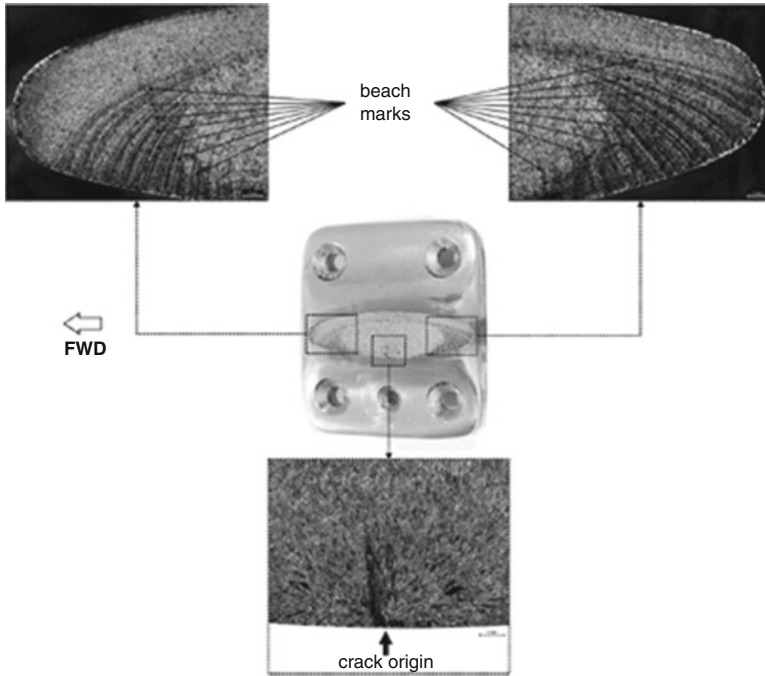
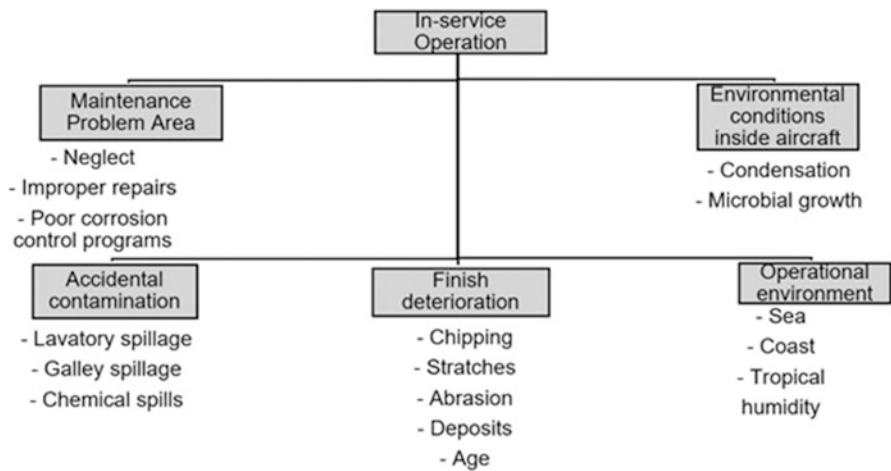**Fig. 3.5** Fractured surface of the ADF antenna (Rebhi et al. 2018)

Fig. 3.6 Common sources of corrosion during in-service operation of aircraft (after Mouritz 2012a)

Corrosion-related expenses are estimated as big as 2.2 billion USD (Mouritz 2012a). It is commonly agreed that if corrosion issues are eliminated, maintenance of aircraft can be simplified. Many sources are available for corrosion during in-service phase of aircraft as illustrated in Fig. 3.6.

Three conditions should be available for corrosion: (i) availability of a reactive metal anode that corrodes and a passive metal cathode (does not corrode), (ii) a metal connector between cathode and anode and (iii) an electrode such as water. Preventing these conditions is quite challenging as it may not be practical, functional and hence feasible to eliminate them. For example, dissimilar metal contact cannot be prevented due to lightweighting, cost and functionality problems. Nevertheless, corrosion potential can be reduced by using surface enhancements such as painting, plating and sealing (Banis et al. 1999). Corrosion types can be categorized as follows:

a. Concentration cell (or crevice, deposit) corrosion: In this type of corrosion, water, moisture or any other pollutant trapped in between two surfaces (e.g. under loose pain, within a delaminated bond line or in an unsealed joint) may lead to pitting or exfoliation corrosion, depending on the alloy, temper and corroded material. Lapped skin joints or rivets on an oil-stained belly are primary spots to notice this type of corrosion.

b. Pitting corrosion: It occurs due to local loss of material. Although small amount of metal is removed, the pits can act as stress concentrators that may result in fatigue failure in critical load paths. Aluminium, magnesium and steel used in aircraft are vulnerable to this type of corrosion.

c. Stress corrosion: This is also referred to as stress corrosion cracking (SCC) or environmentally assisted stress corrosion that occurs rapidly and follows the grain boundaries in aluminium alloys. SCC arises from three factors: susceptible metals and alloys, corrosive environment and residual tensile stress. It is observed on highly stressed parts such as engine crankshafts or landing gears and may originate from a scratch or surface corrosion. SSC occurs in a variety of aerospace metals with the presence of corrosive environment. High-strength steels, heat-treated steels and aluminum alloys are known to be affected by the salt solutions and sea water, and these can cause stress corrosion cracking. Methyl alcohol-hydrochloric acid solutions are reported to cause stress corrosion cracking for some titanium alloys. Magnesium alloys, on the other hand, may stress corrode with moisture in air. It is also reported that sulfur from surrounding environment (e.g., air, dust, or lubricant) can initiate the SCC especially in hot parts (Rossman, 2020). Fig. 3.7f shows SCC failure in 7XXX alloy aircraft wing structure. Reducing the residual and assembly stresses and application of protective coatings are suggested to increase the corrosion resistance and to delay the initiation of SCC for aluminum alloys (Wanhill and Amsterdam, 2010).

d. Exfoliation corrosion: Similar to stress corrosion it follows the grain boundaries and causes a leaf-like separation of the metal grain structure (Fig. 3.7d). It reduces the load-carrying capacity of aircraft parts, and the best way to combat with it is to use material with grain structure resistant to exfoliation.

e. Filiform corrosion: It results from poorly prepared polyurethane paints and appers as worm-like lines under the paint that eventually lead to bubbling and flaking (Fig. 3.7b).
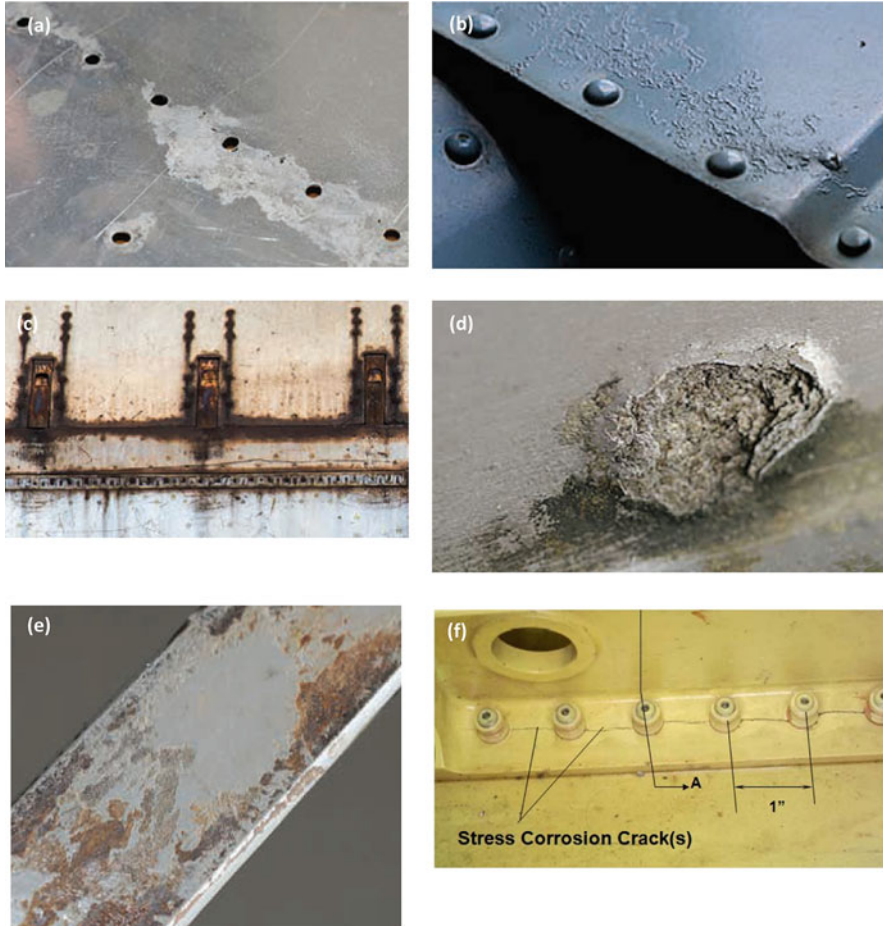
Fig. 3.7 Different forms of corrosion: (a) general surface corrosion, (b) filliform corrosion, (c) galvanic corrosion, (d) exfoliation corrosion, (e) fretting corrosion (Aeronautics Guide, Forms of Corrosion 2019), and (f) stress corrosion cracking (Snyder, 2014)

f. Galvanic corrosion: This type of corrosion occurs by when two metals having different electric potentials are electrically connected via an electrolyte. It can be observed on aluminium–nickel–bronze bushing in an aluminium fitting in macro-scale, whereas one can notice it at the surface of an aluminium–copper interme-tallic in micro-scale (Fig. 3.7c).

g. Fretting corrosion: It is a corrosive attack when two mating surfaces have relative motion with each other, normally at rest. It is characterized by pitting of the surfaces and the generation of fine debris. As the restricted movements of the two surfaces prevents the debris from escaping easily, a highly localized abrasion occurs (Fig. 3.7e).
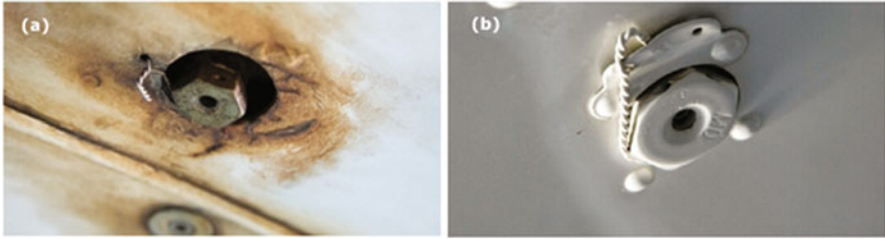
Fig. 3.8 Corrosion marks on different metal parts (**a**) rust around steel bolt, (**b**) whitish/gray dulling on an aluminium surface (Aircraft Owners and Pilots Association n.d.)

h. General surface corrosion: It is the least destructive type of corrosion and also named as uniform surface attack (Fig. 3.7a). As the name implies, the metal is removed from surface uniformly and slowly in this case. Nevertheless, if it is not controlled for a long period, general corrosion may lead to structural failures (Aircraft Owners and Pilots Association n.d.; Mouritz 2012a; Banis et al. 1999).

The visible sign of corrosion for aluminium and steel are quite different (Fig. 3.8). The steel surfaces are covered with reddish colored rust usually while aluminium corrosion is characterized as a whitish or gray 'dulling', which may lead to severe pitting and eventual destruction of the metal.

Trifkovic et al. investigated a failed combat jet aircraft rudder shaft which is a component of the vertical stabilizer (Trifkovic et al. 2011). The function of the vertical stabilizer is to prevent the yawing motion of the aircraft's nose. The components of the vertical stabilizer with rudder shaft are shown schematically in Fig. 3.9.

The rudder shaft made of high strength St. 1.7784 steel failed because of pitting corrosion. Figure 3.10a shows the broken two pieces of the rudder shaft. To see the depth of the pits, the shaft sectioned from the longitudinal crack (shown with number 1), Fig. 3.10b. In Fig. 3.10c, corrosion pits formed in the inner wall are shown with arrows. It can be seen that these pits act as stress concentrators and result in early fracture of the shaft.

Although aluminium alloys provide high strength and fairly high stiffness at a low weight and have been exploited in aircraft structures for years, they are more prone to corrosion and fatigue than any other aerospace material. Corrosion can be minimized, If not avoided, with the selection of the appropriate material, surface finishing operation and the use of drainage, sealants and corrosion inhibitors.

3.1.2.3 Creep

Creep is defined as a process that involves the gradual visco-elastic and/or visco-plastic deformation growth of a material over time, and for metals it occurs at elevated temperature and below the yield strength of the material. The process of creep occurs in three stages: primary creep, secondary creep and tertiary creep.
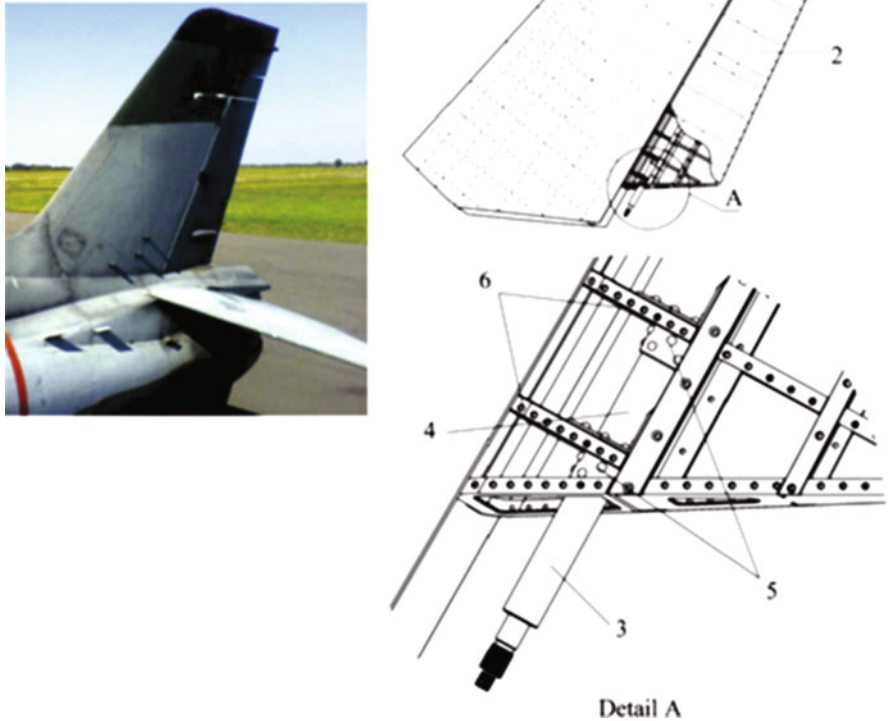
Fig. 3.9 Empennage of an aircraft (on the left) and schematic illustration of the vertical stabilizer-rudder assembly (on the right): *1*. Vertical stabilizer; *2*. rudder; *3*. rudder shaft; *4*. torsional tube; *5*. flange; *6*. rib (Trifkovic et al. 2011)

These stages have distinct behaviours with the function of the time and are illustrated in Fig. 3.11.

Creep is among the encountered failure types in aircraft engine components since those are exposed to extreme temperatures. If a rotating component in the aircraft engine is damaged, it will cause unbalance and lead to high vibration. This sudden increase in vibration can cause destruction in the engine in a very short time. Ejaz et al. conducted a study on the broken aircraft engine. They examined a low-pressure turbine blade made of Udimet 500 (a nickel–chromium–cobalt alloy) and found that primary cracking was initiated on the trailing edge of the blade due to creep; see Fig. 3.12 (Ejaz et al. 2011).

Fig. 3.10 (**a**) Broken
rudder shaft, (**b**)
longitudinal crack formed
on the outer surface and (**c**)
sectioned view of the rudder
shaft (Trifkovic et al. 2011)
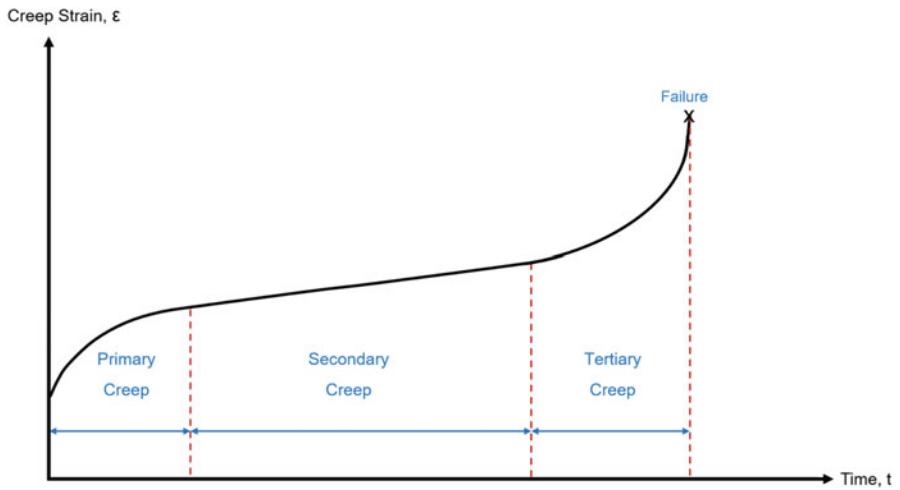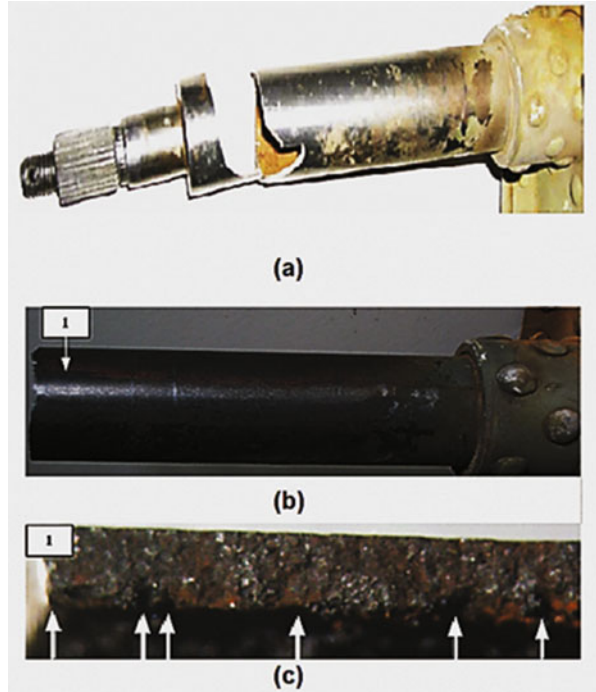
Fig. 3.11   A typical creep curve and its progress

Fig. 3.12 Fractured
low-pressure turbine
blade due to creep (Ejaz
et al. 2011)
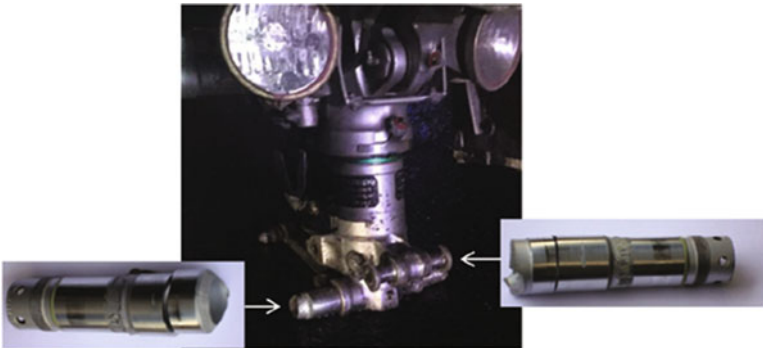
Fig. 3.13 Fractured landing gear (Freitas et al. 2019)

3.1.2.4   Operational Overload

Operational overload failure means that fast fracture of a material when stresses exceed the design stress of a material. Landing gears are the essential parts that undercarriage of an aircraft and are used for both takeoff and landing. It is well known that they are exposed to very high loads, especially at the time of landing. Freitas et al. (2019) showed a failed landing gear in Fig. 3.13. In this case, the aircraft experienced a hard landing due to the severe weather conditions, and the nose landing gear fractured into three pieces. Microscopic examination revealed ductile fracture characterized with dimples on the fractured surfaces (Fig. 3.14). These dimples are the main characteristics of the overloading failures and are due to the coalescence of microvoids during plastic deformation (Freitas et al. 2019).

In aviation, another operational overload type is known as foreign object damage. The sizes of these objects can range from a small solid particle to a wild large bird. Aircraft suffers from bird strikes during any time of flight. This situation is usually attributed to overload damages due to its devastating consequences on the aircraft. It may cause considerable danger to both aircraft and passengers, which can also lead to various major accidents. The number of reported bird strikes to commercial
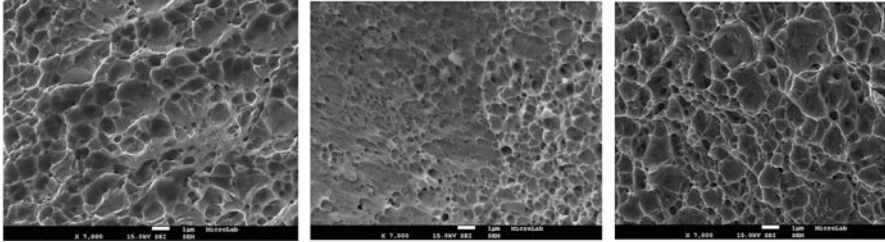
Fig. 3.14 SEM fractographs of the dimples on the fractured surfaces (×7000) (Freitas et al. 2019)
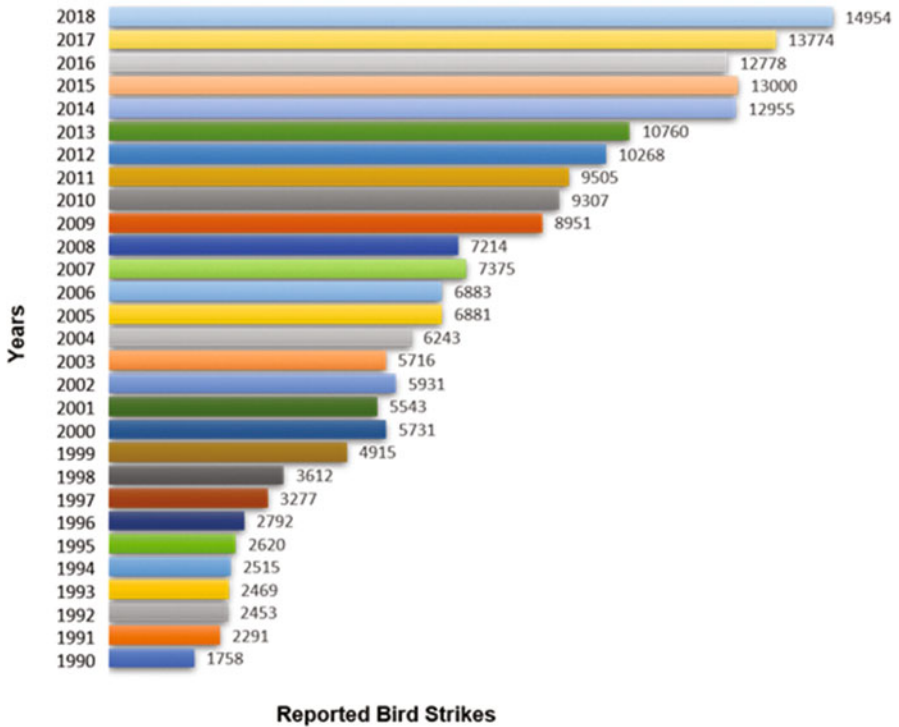

Fig. 3.15 Reported bird hits to civil aircraft from 1990 to 2018 in the USA (Dolbeer et al. 2019)

aircraft between 1990 and 2018 in the United States is given in Fig. 3.15. The number has been increasing over the years. In total, 202,472 bird strikes reported between 1990 and 2018, and almost 16% of these strikes damaged the aircraft (Dolbeer et al. 2019). The specific regions of planes that are susceptible to bird strikes are given in Fig. 3.16.

Figure 3.17 shows some bird strike cases that happened in 2007 and caused significant damages to the aircraft. A black vulture crashed into the nose cone of
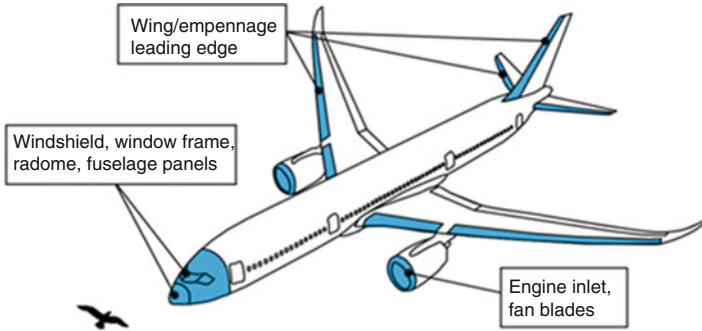
Fig. 3.16 Risky regions for bird strikes (Heimbs 2012)
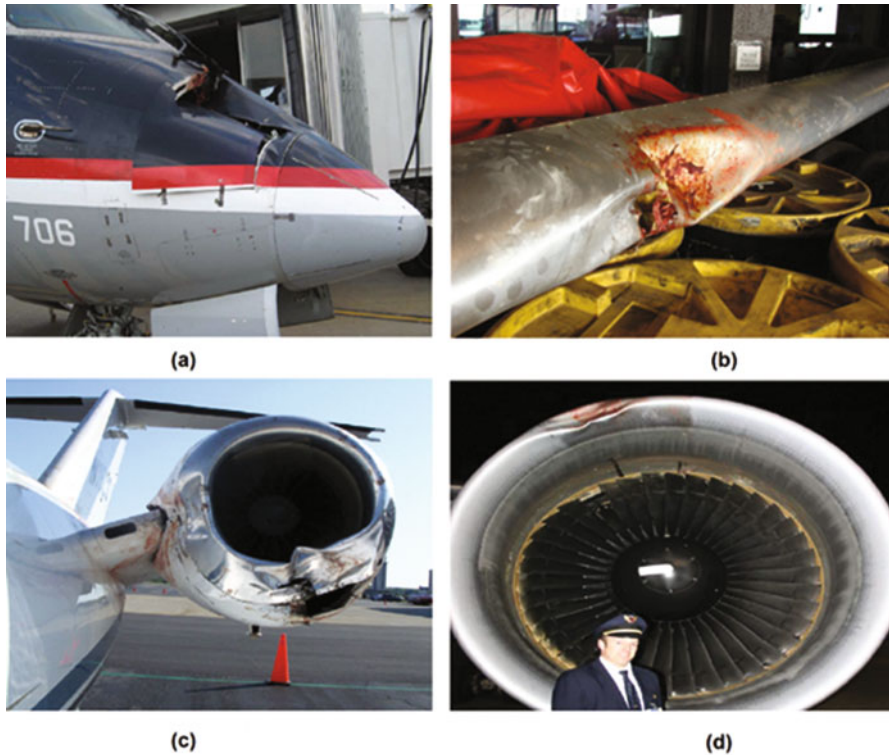

Fig. 3.17 Examples of bird strike aircraft accidents: (**a**) CRJ Jet crashed by a black vulture, (**b**) the leading edge of the left wing of a B-737 hit a great blue heron, (**c**) A Cessna 525 en-route at 5000 feet above ground level was hit by a flock of white-winged scoters and (**d**) a Boeing 767 was struck by a flock of canvasback ducks at 800 feet (Dolbeer and Wright 2008)

CRJ-700 on the final leg to the airport and caused severe damage as it can be seen in Fig. 3.17a. In another instance, a great blue heron struck to the left wing leading edge of the Boeing 737 on approach to the airport (Fig. 3.17b). A flock of white-winged scoters struct to both engines of Cessna 525 at 1500 m altitude (~5000 feet), and engine casing was damaged (Fig. 3.17c). In another instance, a flock of canvasback ducks hit to engines of Boeing 767 at 800 feet. The visual inspection revealed that fan and compressor blades in Engine #1 were seriously damaged (Fig. 3.17d) (Dolbeer and Wright 2008).

3.1.2.5 Wear

Wear is simply defined as some degree of material loss from the surface. These are adhesive, abrasive, fatigue, impact, chemical (corrosive), electrical-arc-induced wear and fretting wear. Erosion is examined under the impact wear and occurs by impingement of sand, rain, volcanic ash and other particles to the aircraft during service. It gradually reduces the life cycle of the components. Particular regions of planes are more prone to erosion on air. Figure 3.18 illustrates these regions. The regions indicated by the smaller dots are exposed to lower speed object impacts and bigger dots are for the medium speed object impacts. The hatched region (nose of aircraft) corresponds to objects with higher speeds (Kutyinov and Ionov 1996).

In engineering applications, bolted parts, shrink and press fits, couplings and bearings are particularly vulnerable to fretting wear. In the aircraft, the most commonly encountered fretting wear occurs in engine components and riveted structural connections. Lee et al. analyzed the failed first-stage compressor blade shown in Fig. 3.19a. In this case, an emergency landing was made due to an engine problem.
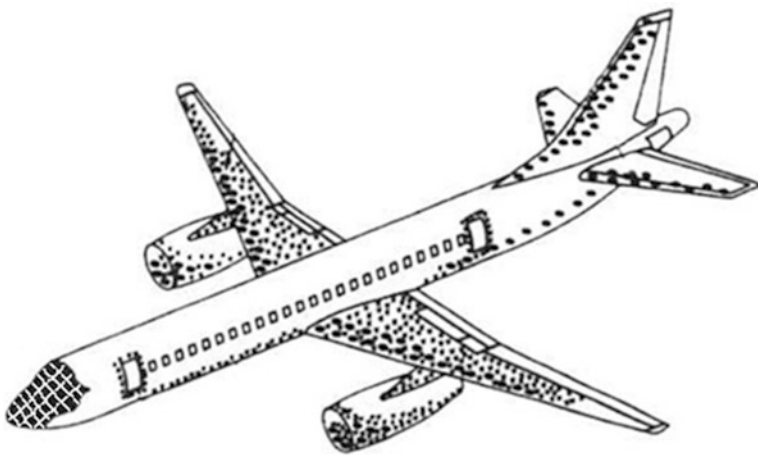
Fig. 3.18 Critical regions for erosion on a commercial aircraft (Kutyinov and Ionov 1996)
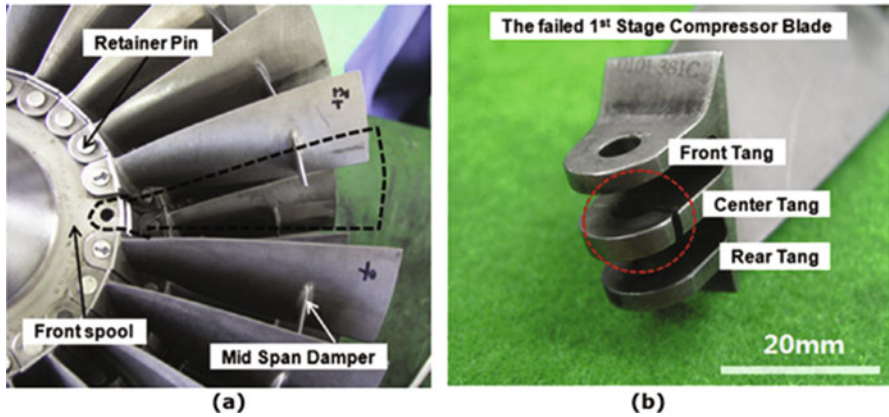
Fig. 3.19 (**a**) Failed compressor blade and (**b**) detailed view of the fractured pinhole lug (Lee et al. 2011)

After a detailed inspection, it was observed that the center tang of a pinhole lag was fractured due to fretting wear induced fretting fatigue (Fig. 3.19b) (Lee et al. 2011).

3.1.2.6 Extreme Weather Conditions

Weather conditions such as low cloud, fog and rain, snowfall, frost, icing, heavy storms (e.g. thunderstorms) and lightning can significantly hamper airline operations, functions of aircraft components and even cause catastrophic damages. Severe weather conditions usually cause increased drag and weight and reduced lift and thrust effect. This section will focus on two of those weather conditions, namely icing and lightning.

Ice is collected primarily on antennas, propeller blades, horizontal stabilizers, rudder and landing gear struts, and it disrupts the function of wings, control surfaces and propellers, windscreens and canopies, radio antennas, pitot tubes, static vents and air intakes. Turbine engines are especially vulnerable as ice forming on the intake cowling constricts the air intake (US National Oceanic and Atmospheric Administration n.d.). Figure 3.20 shows various forms of icing conditions on aircraft parts and a typical deicing operation, which is usually performed by applying heated glycol diluted with water.

Conversely, a lightning strike is an atmospheric discharge of electricity and can cause no damage to significant damage that requires extensive inspection and repair. Today, lightning strikes to airplanes is common yet those rarely result in significant problems due to the lightning protection measures, proper inspection and repair procedures implemented. According to the statistics, a plane can be struck by lightning on average every 1000 to 3000 flight hours. It is equivalent to one strike per commercial aircraft per year (Sweers et al. 2014).
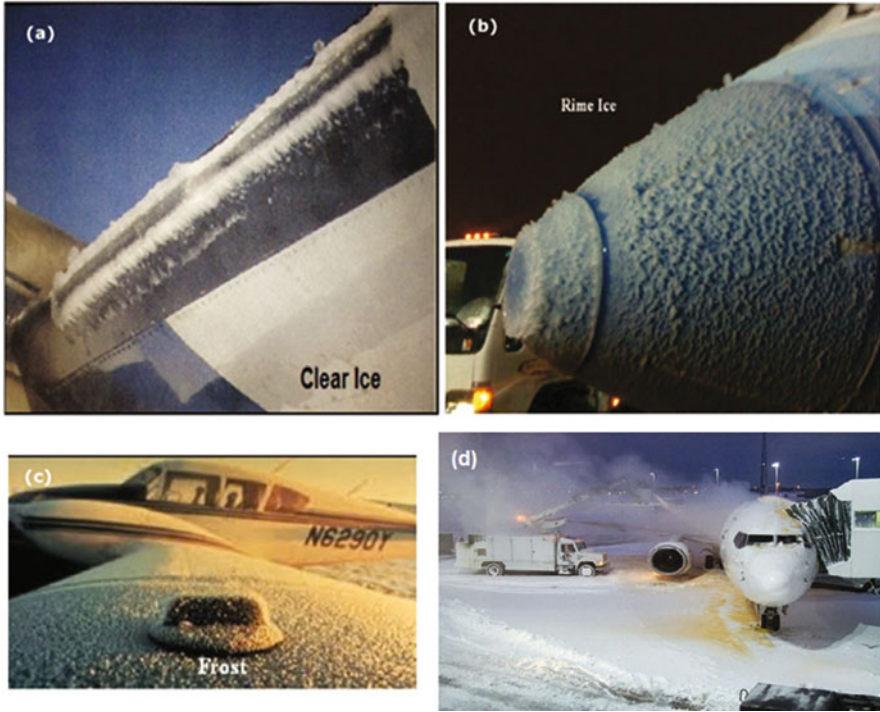
Fig. 3.20 Examples of effect of extreme weather conditions on aircraft: (**a**) clear ice formation on the leading edge of an aircraft wing, (**b**) rime ice on radome of an aircraft, (**c**) frost formation on a wing (US National Oceanic and Atmospheric Administration n.d.) and (**d**) deicing of an aircraft (Hartman 2008)

In 1967, Pan American Airlines Flight 214 was a Boeing 707 flying from San Juan in Puerto Rico to Philadelphia with a stop in Baltimore. The aircraft suffered a lightning strike upon taking off from Baltimore heading to Philadelphia, in which lightning-ignited vapours in the fuel tank led to an inflight explosion, totally destroying the aircraft and killing all aboard. Since then, lightning protection techniques have been improved tremendously. Nowadays, airplanes should be certified to verify the safety of their designs against lightning. As aircraft materials vary, their response to lightning differ. For example, Aluminium is a highly conductive material and, even in the worst-case scenario, the 200,000 A jolt can be quickly conducted away. However, for less-conductive materials such as carbon fibre composites or non-conductive fibreglass, lightning strike protection becomes more critical (Sweers et al. 2014; Black 2013; Rupke 2006). Figure 3.21 shows a lightning damage to a regional jet fuselage.

Fig. 3.21 Lightning strikes damage to a regional jet (Alemour et al. 2019)

### 3.1.2.7 Miscellaneous Defect Types in Metals

Fuselage materials need good resistance against fatigue cracking owing to pressurization and depressurization of the fuselage with every flight (Mouritz 2012a). During pressurization and depressurization of the fuselage, it is highly likely that the materials should be able to carry bending moments, shear forces and torsional loads. If these loads reach a critical limit, the material could have initiation and propagation of cracks leading to catastrophic failure of the fuselage structure. Overall, fuselage materials require a combination of properties that include lightweight, high elastic modulus and yield strength and resistance against fracture, fatigue and corrosion. Among metallic materials, high strength aluminium alloy is the most common fuselage materials. The new generation of Al–Li alloys is a modern metallic material used in the production of aircraft parts, such as fuselage sub-assemblies or floor bearing elements (e.g. A380). These alloys are characterized by attractive mechanical properties in comparison to conventional aluminium type alloys. The Al-Cu 2xxx series alloys, characterized by high strength and low-density properties, as well as Al-Zn 7xxx series alloys characterized by high corrosion resistance, are used for structural applications, such as aircraft wings. The development of light-weight materials and fabricating parts/sub-assemblies of substantially large dimensions has become a major issue for the aerospace industry, which has boosted the development of more advanced materials with high specification properties. Recent aluminium alloy developments are based on achieving superior fatigue crack growth resistance, better corrosion resistance, lower density etc. Standard manufacturing techniques, such as welding and casting or extrusion, are ought to be developed to find a beneficial solution allowing structural weight reduction.

Aluminium alloys used in aircraft applications possess several extraordinary properties that make them suitable for use in the manufacture of the structural parts of aircraft. Extrusion as a manufacturing process of these materials allows for

the obtaining of the required quality of the specific geometrical parameters, macro- and micro-structure, properties (including mechanical ones) but also creating structural elements of very complex cross-sections, whose manufacture is usually impossible or more costly with the use of other techniques. Another main advantage of this process is its ability to select optimum shapes of extruded blanks used to manufacture parts maximally similar to the theoretical profile of the final part. Aluminium is the most commonly extruded material. Examples of products include profiles for the following aircraft parts: brackets, levers, fasteners, frames, liners, window frames, rails and cargo (Pawłowska and Śliwa, 2015). Although profiles production in extrusion runs smoothly and easily most often, several repeated faults might occur during the extrusion process and some distinct patterns of faults and defects can be seen on the surface of the produced profiles (Al-Jabbouli et al. 2015). To avoid possible defects in the extruded profiles (e.g. damage of the finished surface, internal or external cracks, banding of extruded profiles) the extrusion rates have to be selected not to cause any damage to the finished surface, which would prove the disturbance of the extrusion process or negative structural phenomena in the material (e.g. hot cracking).

Wings are designed to carry bending, shear and tension loads. During take-off, flight and landing stages, the bending action on the aircraft wing, which is a combination of tension and compression forces, including fluctuation of loads can induce fatigue damage. Among metallic materials, aluminium alloy is used to make wings, whereas the wing-box and wing connections are highly loaded structures built into the fuselage that are constructed of composite material or titanium alloy (Mouritz 2012a).

Undercarriage materials (e.g. landing gear) are expected to have high static and dynamic strength, fracture toughness, including fatigue strength. Arguably, the most used materials for load bearing part in aircraft is high-strength steel. The critical components of one of the largest landing gear assembly in commercial service (Airbus Industrie A330 and A340 passenger aircraft) are made from tempered martensite (Bhadeshia 2006). As an example, Fig. 3.22 contains the micro-structure
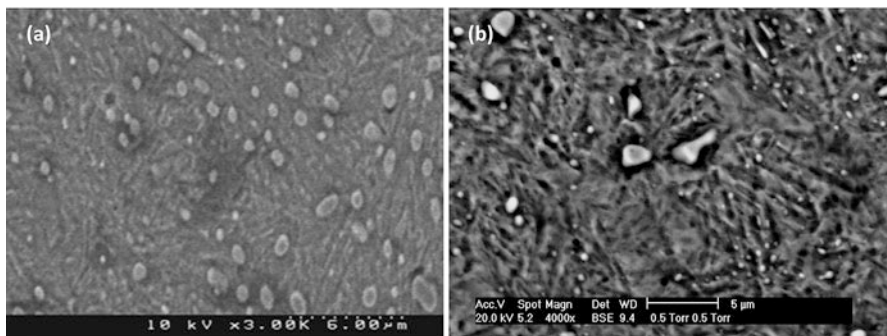
Fig. 3.22 Martensitic steel surface (polished and etched surface) showing lathes and coarse carbides, with dark zones or microvoids between carbide particles and martensitic matrix (Faisal et al. 2011b)

of the high strength hardened steel showing spheroidal carbide particles dispersed in a martensite matrix phase, which itself probably contains some smaller temper carbides. Small spheroidal carbides observed in Fig. 3.22 or many high-carbon martensite structures are considered routine (Faisal et al. 2011a). However, grain-boundary carbides, massive carbides that occur on edges and corners are deemed detrimental to mechanical properties and should be avoided. While carbides are harder than the surrounding matrix (martensite/austenite), they do not always have an appreciable effect on micro-hardness (e.g. Vickers or Rockwell). Carbides are known to enhance wear resistance.

In the high-strength hardened steel, the carbides are much harder than the tempered martensitic surrounding matrix so that any plastic deformation gets concentrated in the surrounding matrix and is impeded by the carbides (Blaha et al. 2002), leading to an accommodation mechanism including plastic deformation and carbide cracking (Girodin et al. 2002). The details of this failure mechanism may not be visible at the microscopic magnifications normally used in conventional material testing and optical analysis, although some evidence of failure at the carbide–matrix interface can be visible for some of the larger particles using acoustic emission (AE) sensors during contact mechanics study (Faisal et al. 2011a) (e.g. Fig. 3.22).

Since no macro-cracks can easily be detected on the surface around the stressful zones (tensile or compressive during contact mechanics), it is expected that the fine distribution of the brittle phase leads to generate micro-cracking in the areas of highest tensile stress (Faisal et al. 2011b). Since the stress is tensile over the entire contacting edge (e.g. indentation loading), it is expected that micro-cracking will initiate or be present in these areas.

Materials used in gas turbine engines are required to operate under high stress and temperature conditions for long periods of time (Mouritz 2012a). Engine materials require a combination of properties that includes high strength, toughness, fatigue resistance and creep strength at elevated temperature. Engine materials must also resist damage from oxidation and hot corrosive gases. The material of choice for the hottest engine components are nickel-based superalloys.

3.2   Composite Materials

Composites are of growing importance in aeronautics. They offer explicit weight saving in comparison with metal parts together with high quality and resistance to fatigue and corrosion. The modern, optimized composite aircraft structures require careful monitoring and inspections to identify damage and take corrective action as needed to ensure continued safe operation. The constant aggravation in quality requirements for aeronautics makes the defect detection and NDI techniques of prime importance, both in manufacturing and in-service inspection.

All the main types of composites such as polymer, ceramic and metal matrix composites (PMC,CMC, MMC), hybrid composite and structural composites (laminar composites, sandwich panels) demonstrate different mechanical and structural
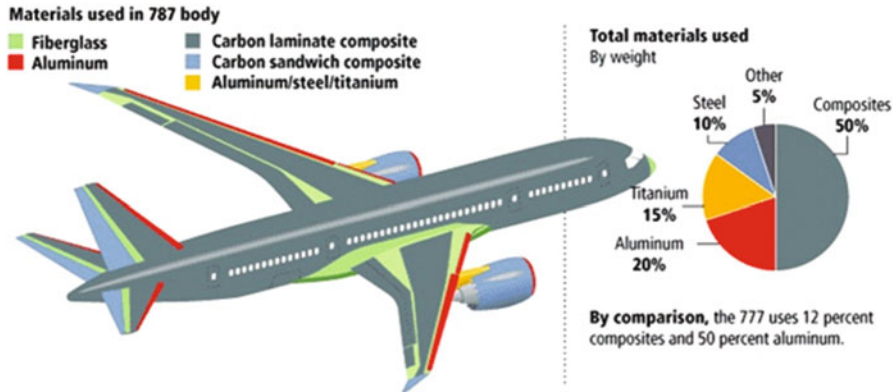
Fig. 3.23 Composites and other structural materials used in aircraft construction. Example: Boeing 787 body (Rosato 2013)

behaviour in special current and future applications in the aerospace industry. Recently, fibre-reinforced polymer composites are developed and used in the aerospace, especially carbon- and glass-fibre-reinforced plastic (CFRP and GFRP respectively) that consist of carbon and glass fibres, both of which are stiff and strong (for their density), but brittle, in a polymer matrix, which is tough but neither particularly stiff nor strong. Metal and ceramic matrix composites remain important materials, e.g. fiber metal laminates, in particular glass fiber reinforced aluminium laminates (GLARE) of high fatigue performance or carbon-carbon (CC) composites as ceramic matrix composite for high temperature applications. An example of *use of composites in aircraft design* is presented in Fig 3.23.

Composite materials have been used in the aerospace industry in primary and secondary structural parts, including rocket motor casings, radomes, antenna dishes, engine nacelles, horizontal and vertical stabilizers, centre wing boxes, aircraft wings, pressure bulkheads, landing gear doors, engine cowls, floor beams, tall cones, flap track panels and so on. The use of advanced composite materials in the aerospace sector is growing due to several advantages of composites over metals, such as composites light weight, high strength, corrosion resistance and superior fatigue and fracture properties, as well as multifunctional performances such as SHM and self-healing.

The major aspects related to quality control during composites manufacturing and their maintenance, testing and repairing in services: visual, ultrasonic, X-ray, back light and moisture detectors are some of the techniques reviewed as the main methods commonly used to detect damages, e.g. in sandwich structures that are applied in aerospace and aircraft parts. Major manufacturing damage and defects usually include delamination, resin starved and resin-rich areas, cracks, blisters and air bubbles, wrinkles, voids and thermal decomposition.

The following subsections describe the major defects encountered in composites. For each defect, we will explicitly indicate whether it is a manufacturing, an in-service or both a manufacturing and in-service defect.

3.2.1   Disbonds

Disbonds are both manufacturing and in-service defects. They are defined as unplanned non-adhered or unbonded areas within a bonded interface. They can be caused by adhesive or cohesive failure and may occur at manufacturing or at any time during the life of the structure. Disbond is generally a result of misprocessing during manufacturing such as incorrect initial surface cleaning, pressure/vacuum fail or an excessive load of the structure during service. Actually, this type of damage is dependent on the integrity of the adhesive layer and is affected by the presence of manufacturing defects as well as in-service loads. Manufacturing defects include a wide range of misprocesses such as poor surface preparation, contamination, improper curing, inaccurately applied pressure, the geometrical mismatch between the adherends and trapped air/moisture in the adhesive mixture.

Poor surface preparation is one of the leading causes of adhesively bonded joint failures. The creation of porosity and voids can also degrade the adhesive properties, as well as, create stress concentration during loading. During service, disbond can occur due to excessive stress applied at the bonding interface, impact damage, environmental degradation such as moisture ingression and aging of the adhesive layer (US Department of Transportation, FAA-AR-09-4 2009 (Tomblin, Seneviratne and Pillai, 2009)). Disbond can be found in any bonding surface, some of the examples include laminate/metal or laminate/laminate bonding surface, laminate skin to core (honeycomb or foam) bonding surface in sandwich structure and core to the core in multiple sandwich structure. Typical disbonds are shown in Figs. 3.24, 3.25, 3.26, and 3.27.
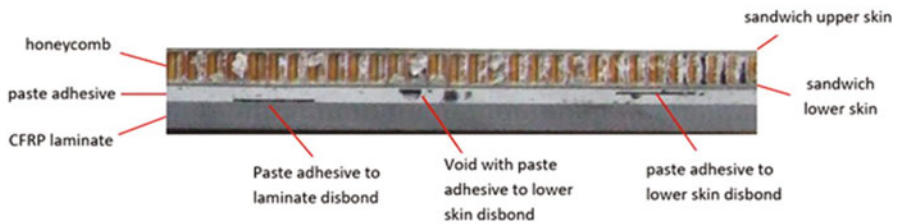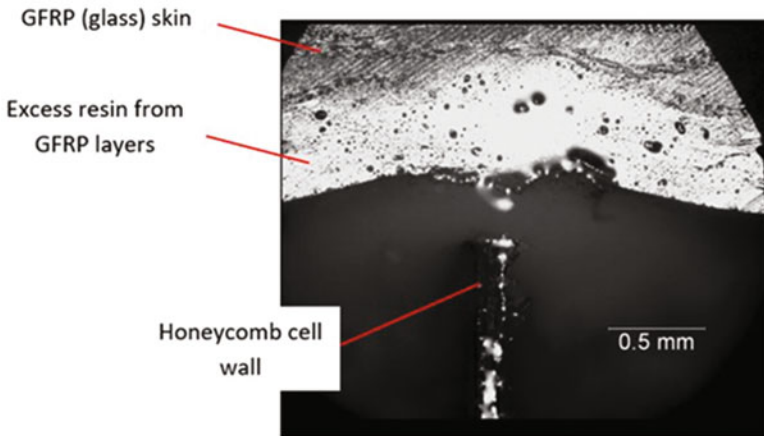

Fig. 3.24 Section of honeycomb sandwich structure bonded to CFRP laminate (either spar or rib) by paste adhesive showing several disbond issues
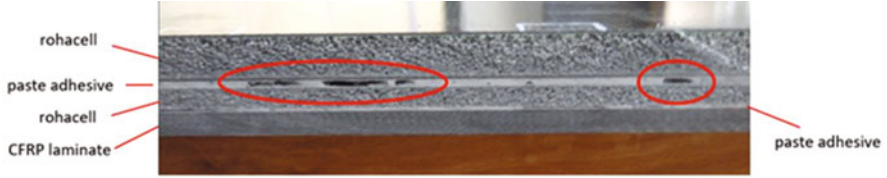
Fig. 3.25 Section of ROHACELL® foam blocks bonded together showing several disbond defects at the interface line
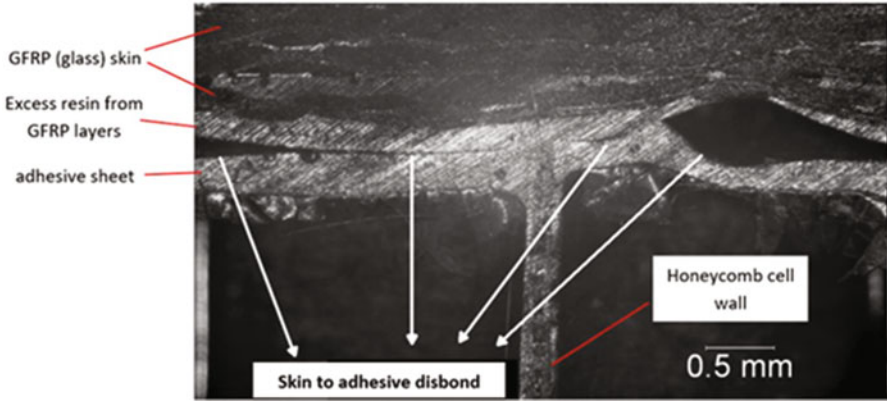
Fig. 3.26 Honeycomb sandwich structure—disbond between the adhesive layer and the GFRP skin

Fig. 3.27 Honeycomb sandwich structure - disbond between the honeycomb cell wall and the GFRP skin, and porosity bubbles are also visible within the excess resin
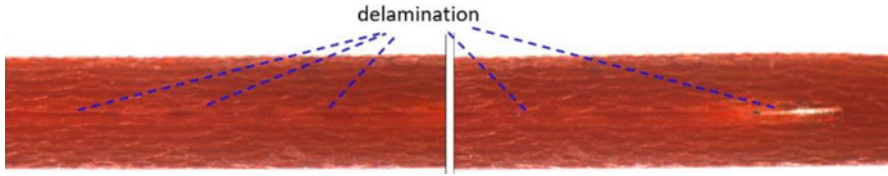
Fig. 3.28 Stereoscopic microscopic view of delamination within a GFRP laminate
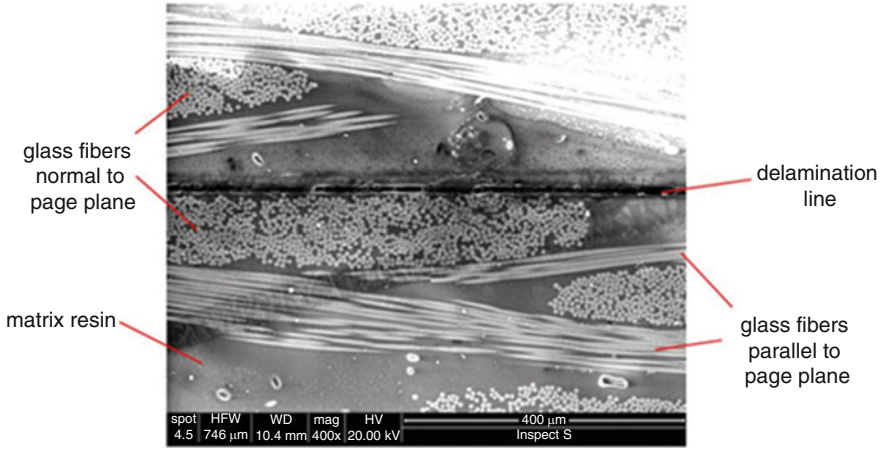
3.2.2 Delamination

Delaminations are both manufacturing and in-service defects. In composites, they can be defined as a local failure in the adhesion between two successive layers causing the two layers to separate from one another at that location. Delamination can be caused by misprocessing during manufacturing (such as pressure/vacuum failure) or by impact damage or excessive load during in-service. Delamination is caused due to matrix properties having lower fracture toughness, strength and resistance against inter-laminar shear and transverse tension as compared to the reinforcement constituent. During the manufacturing process, thermal stresses and resin cure shrinkage can give rise to residual/inter-laminar stresses. These stresses can be high enough to cause delamination due to the mismatch between the properties of two adjacent layers (Bolotin 1996).

In-service delamination may be due to temperature cycling, local loads, impacts and fatigue. Failure due to delamination often initiates from free edges, surface defects and stress concentration points, which leads to the loss of overall stiffness/strength and under compressive loading leads to reduced buckling load limits (Vorontsov et al. 1990). Delaminations can also occur at free edges, in which a local three dimensional stress state phenomena plays an important role. Mainly explained by the mismatch of the elastic material properties between two adjacent dissimilar laminate layers, the free-edge effect is characterized by the concentrated occurrence of three-dimensional and singular stress fields at the free edges in the interfaces between two layers of composite laminates (Mittelstedt and Becker 2007). Several delamination cases are shown in Figs. 3.28, 3.29, and 3.30.

Defects in the composites may also occur during other processes, e.g. during drilling (Figs. 3.31 and 3.32), where delamination and extracted fibres are visible (Tyczynski, Śliwa, Ostrowski 2015).

3.2.3 Foreign Inclusion

Foreign inclusion is a typical manufacturing defect. It stands for the presence of a foreign body within the composite structure. Generally, foreign inclusions are pieces of material that have inadvertently not been removed from the surface before bonding. Most foreign inclusions in composites are the remains of unremoved pieces of: (a) protective sheets of preimpregnated plies, either paper, nylon or teflon sheets,

Fig. 3.29 SEM view of delamination within a GFRP plain weave laminate; Average fibre diameter is 5–7μm
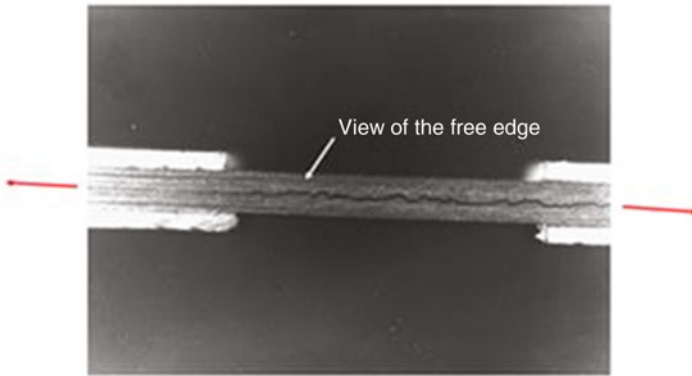
Fig. 3.30 Free edge delamination of a $[0_2, +45, 0_2, -45, 0, 90]_s$ laminate under tension loading
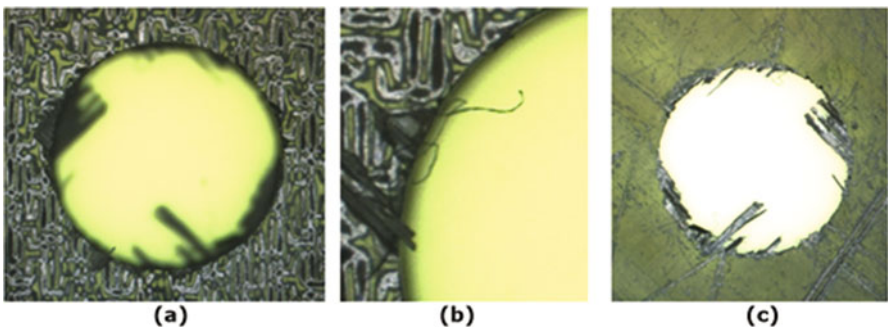
Fig. 3.31 Drilling of composite GFRP: Input (**a**, **b**) and output (**c**) surface of the hole with clearly visible delamination and extracted fibres
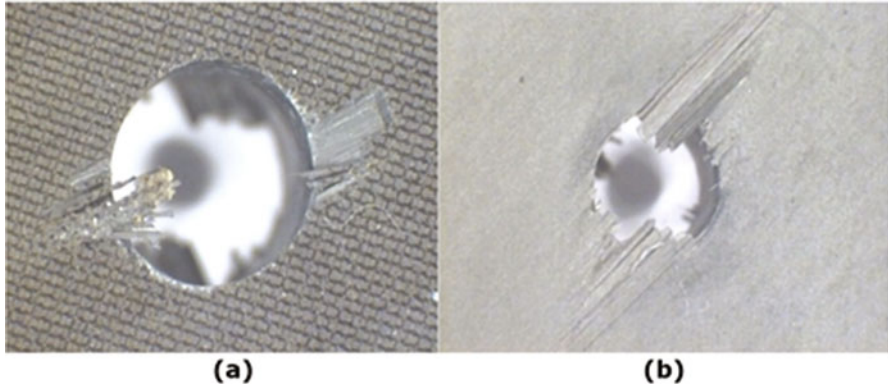
Fig. 3.32 Delamination in a carbon composite CFRP: (**a**) multidirectional (**b**) unidirectional
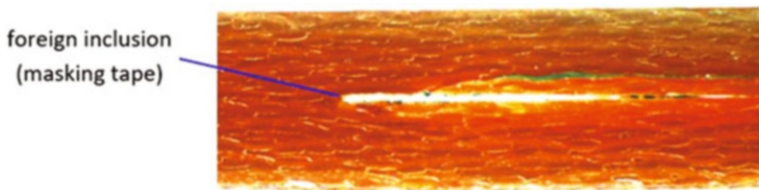
Fig. 3.33 Stereoscopic microscopic view of foreign inclusion (masking tape remaining) within GFRP laminate
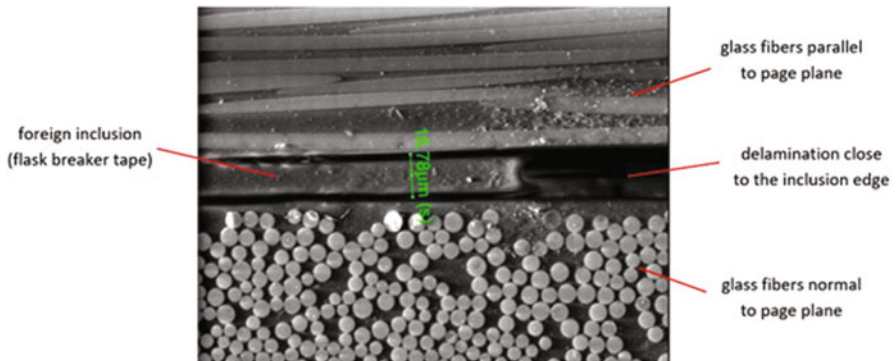
Fig. 3.34 SEM of foreign inclusion (flask breaker tape remaining) within a GFRP laminate; The upper ply has glass fibres oriented in the plane of the picture, whereas the lower glass ply has fibres normal to the picture plane. The average fibre diameter is 5–7μm

(b) masking tape, (c) flash breaker tap and (d) peel ply that is an extra layer of synthetic material (glass, nylon or other) which is laid upon the outer surface of the composite during fabrication. This layer is intended to be peeled off in a subsequent bonding step before bonding. Several foreign inclusion examples are shown in Figs. 3.33 and 3.34.
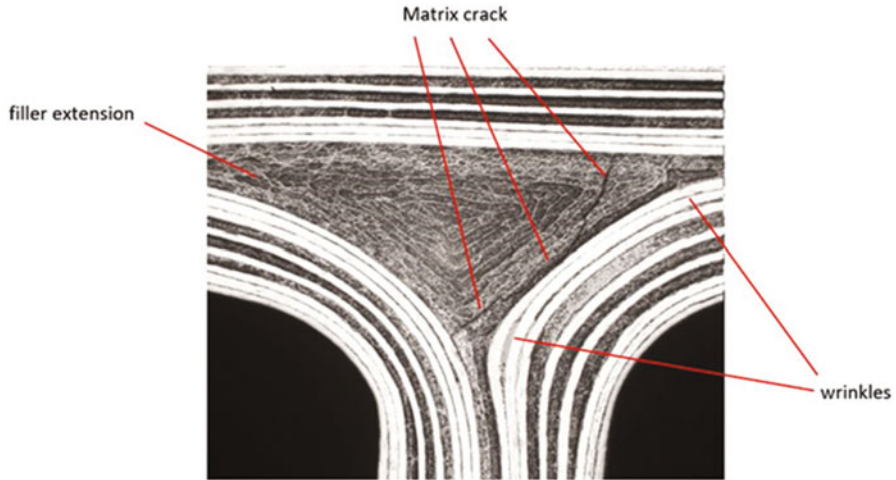
Fig. 3.35 Interfiber matrix cracking in CFRP T-shape radius filler made of unidirectional graphite fibres embedded within resin; The part that experienced a misprocess during fabrication is geometrically distorted and shows besides the crack two wrinkles on the right side and filler extension on the left side

3.2.4 Matrix Cracking

Matrix cracking is both a manufacturing and in-service defect (Fig. 3.35). It is characterized by cracks within the resin cementing the fibres of a laminate structure. It is often caused by mechanical stress lateral to the direction of the fibres, either during manufacturing or in-service. It is usually the first damage to occur when a composite laminate is subjected to mechanical stress such as quasi-static/cyclic tensile loading (Gayathri et al. 2010). Matrix cracking is characterized by damage in one or more layers without reaching the opposite surfaces. It turns into 'fracture' when the damage extends through the entire layers of the laminate.

During manufacturing, matrix cracking is often a consequence of thermal and/or residual stresses. It occurs in the through-thickness and transverse directions and can run perpendicular and parallel to the fibres, respectively. The through-thickness cracks occur because of the significantly lower matrix strength/stiffness as compared with the reinforcement and the strain magnification within the matrix pockets. Similarly, transverse cracks appear due to a mismatch between the in-plane Poisson's ratio of the plies in the loaded and off-axis directions (Abrate 1991). This type of damage usually occurs during service as a result of tensile, fatigue and impact loading and is affected by the polymer matrix (Hu 2007).

Improper curing is a matrix-dominated defect because during the cure cycle the resin changes its physical state from liquid to rubbery to glassy. Incomplete/non-uniform curing creates parts with thickness variation causing residual stress to build up, thus affecting the stiffness and toughness of the composites, whereas over-curing

can lead to matrix cracking or burning. Improper cure can also entrap volatiles, which can lead to void formation (Antonucci et al. 2006).

Mechanical processing steps such as drilling, trimming and machining can introduce inter-laminar matrix cracking. Matrix cracking can affect moisture absorption by providing more space for the moisture to penetrate the laminate. It can also act as a stress concentration point that causes the part to fail.

3.2.5 Porosity

Porosity in composites is a manufacturing defect caused by incomplete gas microbubbles outflow from the part during the process. A part of the microbubbles that should leave the part remains stuck to the layers and/or bonding interfaces and often combine to form discrete bubbles (Fig. 3.36). The discrete bubbles themselves can also combine and lead to macroscopic delamination or disbond. Porosity is generally defined per volume percentage. High porosity level (several percent) critically affects mechanical properties and thus aviation companies tend to severely limit porosity level to low values on critical parts (1.5% or 2% maximum). When the porosity level is high, the individual gas microbubbles often merge into voids. Actually, porosity and voids affect compressive, shear and bending strengths, which are dominated by the matrix properties. They also act as stress concentration points and possible damage initiation sites (Rubin and Jerina 1995).
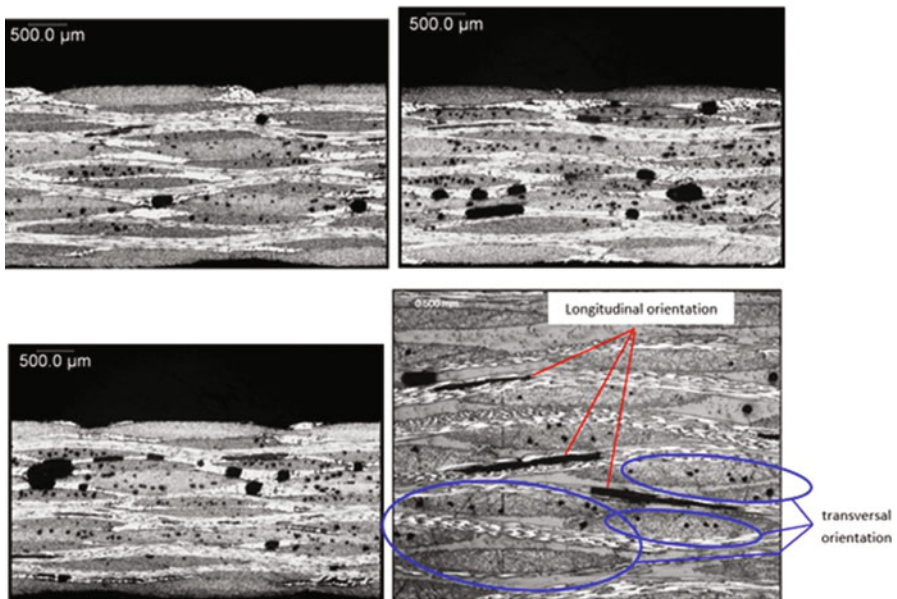
Fig. 3.36 Sections of CFRP laminates with porosity. Porosity bubbles tend to align with fibre orientation and thus often appear either in transversal or longitudinal direction

3.2.6 Fibre Breakage

Fibre breakage occurs when the applied stress is greater than the fracture strength of the fiber. Typically, failure due to fibre breakage occurs in steps. First, the fibre with an existing damage fails, which in turn, increases the load concentration in the surrounding intact fibres. Since the load distribution is now higher for the remaining fibres, the next weakest fibres tend to fail. This process will repeat until the entire structure fractures. Fibre breakage is generally caused in-service due to foreign-object impact, lightning strike, applied load, erosion, scratches and abrasion.

3.2.7 Other Composite Laminate Typical Defects

Apart from the defects mentioned above, composite laminate may have other defects such as non-uniform laminate thickness and wrinkles or waviness. Non-uniform laminate thickness is a typical manufacturing defect generally related to non-uniform pressure or moulding tool misplacement during fabrication. An example of non-uniform laminate thickness in radius is shown in Fig. 3.37. Wrinkles (waviness) is also a typical manufacturing defect generally related to uncontrolled layer displacement during processing. Wrinkles can significantly affect the mechanical properties of composite laminates. A typical laminate wrinkle in a radius is shown in Fig. 3.38. Waviness can be formed during the cool-down phase of composite
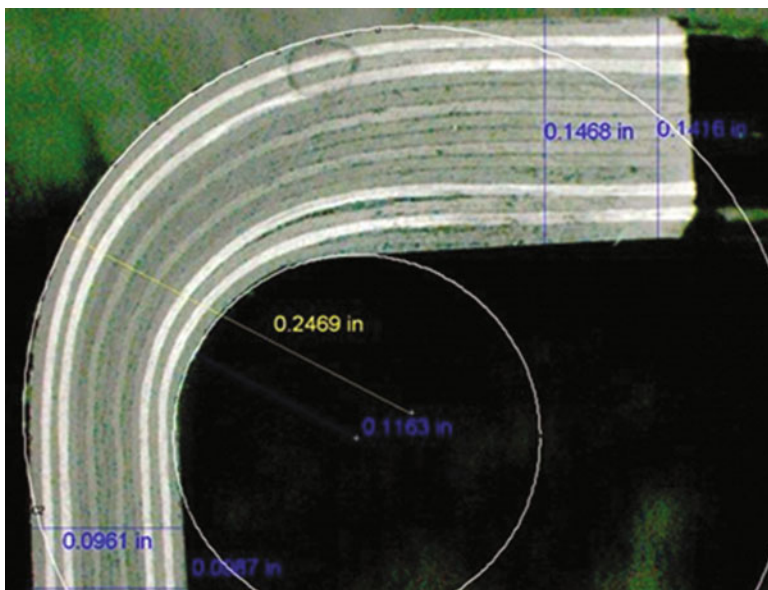
Fig. 3.37 Laminate non-uniform thickness in composite CFRP radius

Fig. 3.38 Laminate wrinkles in composite radius

manufacturing due to a mismatch in the thermal expansion between fibres and matrix and/or composite part and the tool plate (Kugler and Moon 2002). Also, during the fabrication stage, the lamina oriented in different directions attempts to slip with respect to one another. If this slippage is restricted by the neighbouring plies, waviness can form (Vanclooster et al. 2009). Because of waviness, shear stresses can be induced because of the offset angle between the fibres and the applied load. This shear stress produces shear strains, which leads to greater misalignment of fibres. Therefore, waviness reduces the compressive strength of a composite (Wisnom 1993).

3.2.8   Typical Honeycomb Core Defects

Apart from honeycomb to laminate disbond mentioned above, honeycomb cores may also suffer additional defects (see Figs. 3.39, 3.40, 3.41, and 3.42) that may occur both at manufacturing or in-service steps as defined: (a) honeycomb to honeycomb disbond in multicore structures, (b) condensed core that is a lateral distortion of the size of the cells relative to their axis, (c) buckled core that is a general lateral shift of the cells relative to their axis, (d) crushed core that is a collapse of the core parallel to the cell axis and (e) torn core that is characterized by cell breaking in a perpendicular direction to the cell axis, and this defect is often related to excessive core crushing.
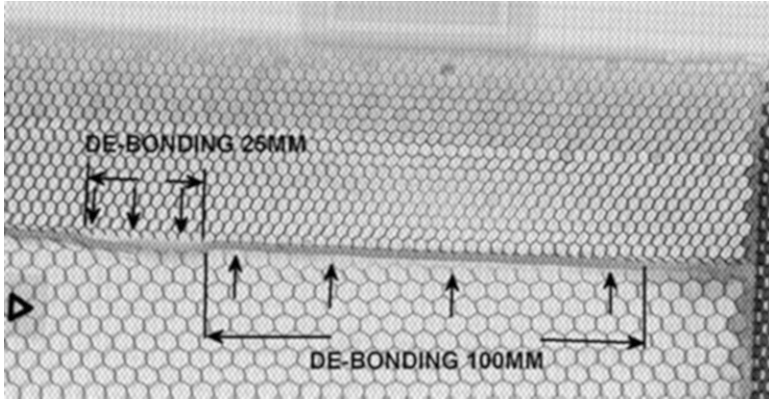
Fig. 3.39 X-ray radiography of honeycomb core to core disbond
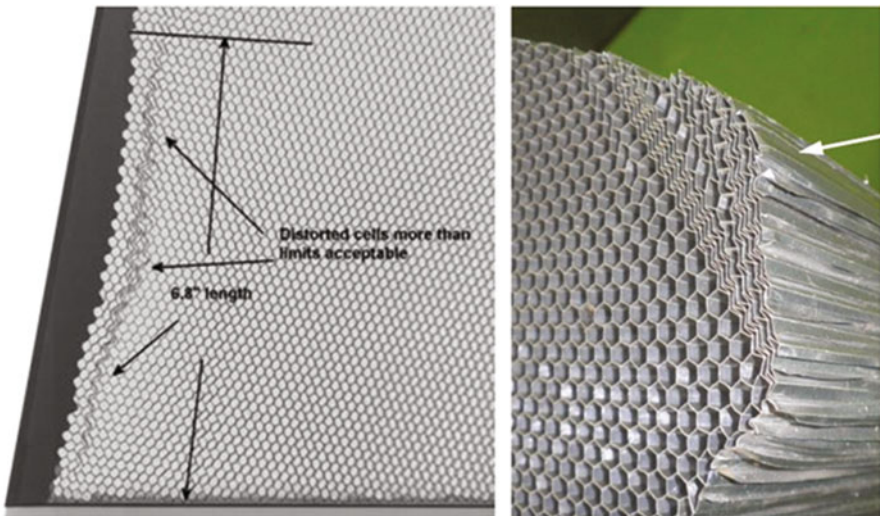
Fig. 3.40 X-ray radiography and visual examples of condensed honeycomb cores

3.2.9 Typical Foam Core Defects

Apart from foam to adhesive disbond defects mentioned above, foam cores may also experience other types of defects that may occur (see Fig. 3.43) both at manufacturing and in-service steps as defined: (a) core cracking that is generally related to excessive stress applied to the core and (b) core subsurface cracking that can be considered as a typical foam disbond defect. Since at bonding surface involving foam cores, an adhesive is always showing some slight penetration within the foam (less than 1 mm in thickness), the disbond appears within the foam just below the adhesive penetration line rather than at the foam limit line.
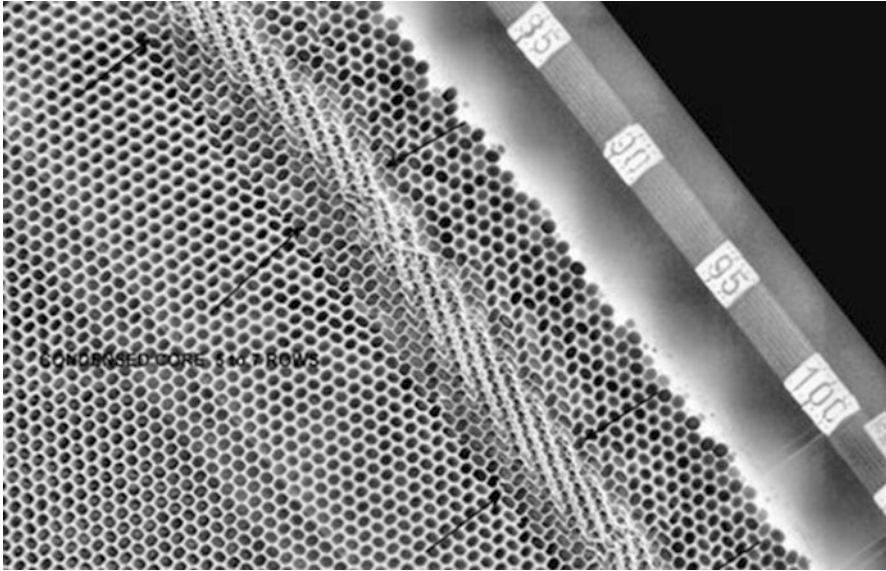
Fig. 3.41 X-ray radiography and buckled honeycomb core

Fig. 3.42 X-ray radiography and torn honeycomb core
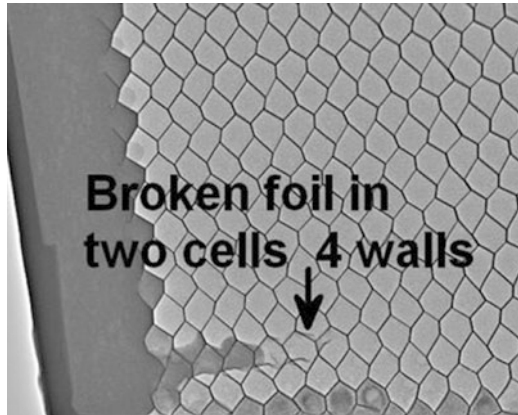
3.2.10 Ingress of Moisture and Temperature

The material properties of fibre composites are also influenced by moisture and temperature. The effect is notably large at higher temperatures and moisture. Figure 3.44 shows the effect on the material properties obtained on small specimens (T300, fiber volume fraction = 0.6, 914C). The matrix 914C is one of the first generation used in aerospace. However, the general behaviour for different resin systems is similar.

A: Outer skin
B: Rohacell foam upper limit mixed with adhesive
C: Subsurface Rohacell foam cracking line
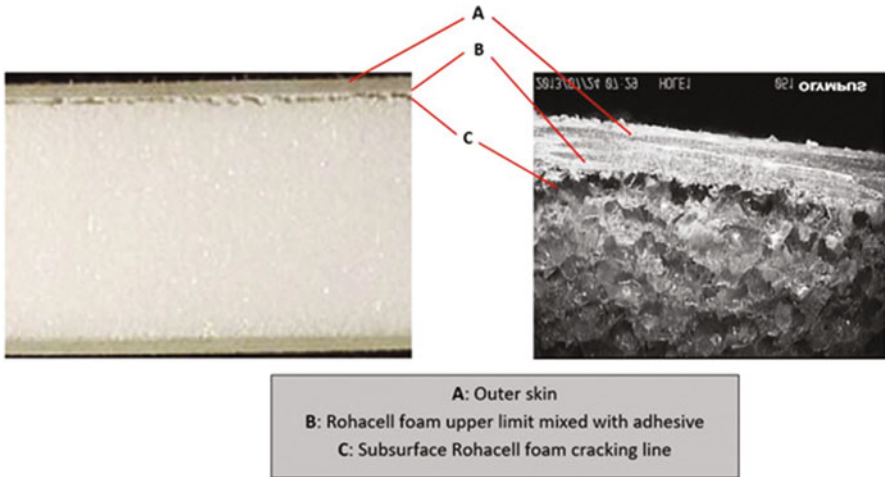
Fig. 3.43 Rohacell foam core subsurface cracking; This is a typical foam core disbond. Disbond appears below the actual Rohacell foam to skin interface as subsurface cracking rather than at the rohacell foam outer limit that is mixed with an adhesive
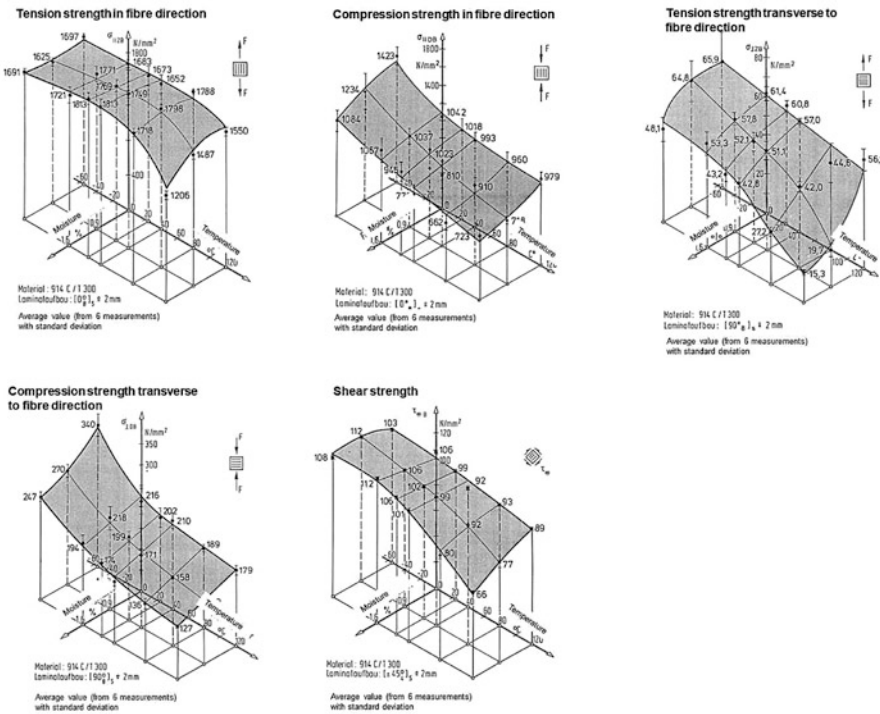
Fig. 3.44 Influence of moisture and temperature on the material properties (T300, phi = 0.6, 914C) (Gädke 1988)

3.2.11 Fatigue

Fatigue is the weakening of a material caused by cyclic loading that results in progressive and localized structural damage and growth. In metallics, the growth of cracks is considered. Fibre reinforced composites shows three phases of damage growth: (a) onset of first matrix cracks. With the growing number of cycles, the crack density increases and gets more compact. Crack density reaches its saturation level when the characteristic crack pattern is reached, (b) formation and growing of delamination and (c) buckling of delaminated areas and degradation until collapse. Different examples of fatigue loaded structures are as follows.

Figure 3.45 illustrates the characteristic crack pattern of a $[(0, +45, -45, 90) 2]_S$ laminate under R $= -1$ fatigue loading. Although the panel looks quite damaged the residual strength is still 85%. Figure 3.46 shows the influence of small impact damage on damage tolerance. For the static case, the influence of strength is reduced significantly to about 30-40%. However, under fatigue loading, these values are almost constant and only very slightly reduced to 25% strength, which is very damage tolerant. This behaviour is different from metallics where the influence of cracks is smaller for the static case and much larger for the fatigue loading. Figure 3.47 shows the fatigue behaviour of a $[0_2,+45,0_2,-45,0,90]_S$ laminate with an artificial delamination of ø10 mm in the middle of the plate. The stress amplitude is ±400 MPa and the stress ratio R $= -1$. The number of cycles until collapse is reached at 14.2×10^4. It can be seen that the artificial delamination is almost no growing until collapse. However, there are more delaminations at the edges due to the free edge effects. Figure 3.48 shows the results of a stiffened CFRP panel cyclically loaded by axial compression. The panel was partly artificial pre-damaged by separation of the second stringer by a Teflon layer. In each cycle,
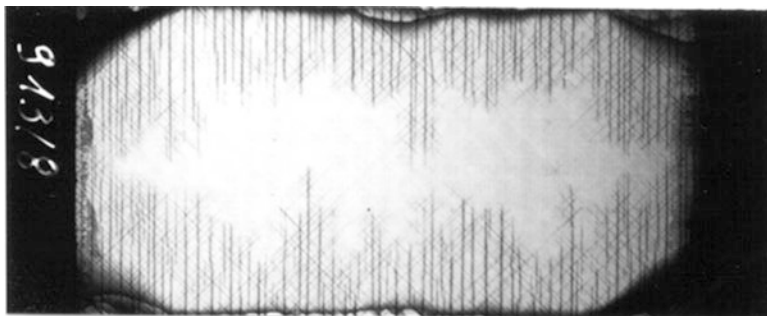
Fig. 3.45 Characteristic crack muster of a $[(0,+45,-45,90)2]_S$ laminate under R $= -1$ fatigue loading which still has 85% of residual strength
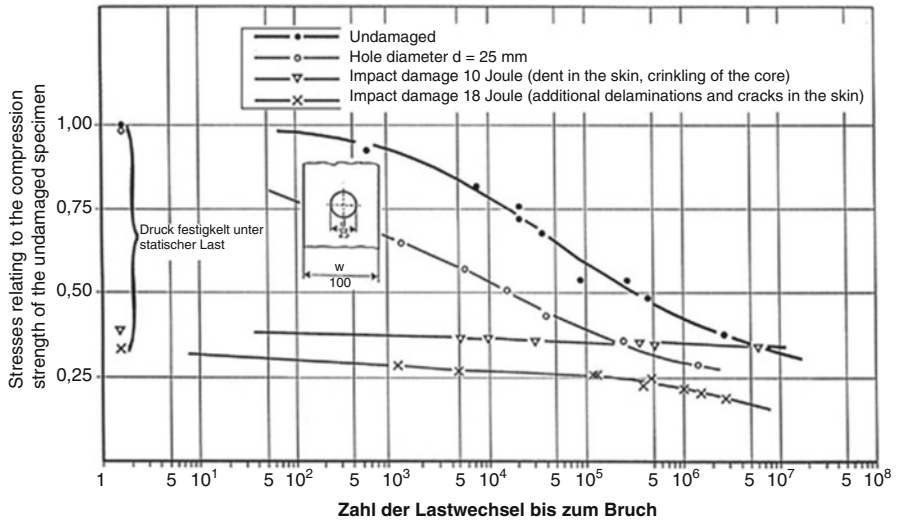
Fig. 3.46 Fatigue behaviour of a sandwich structure, R = −1, f = 5 Hz, Skin: GFRP fabrics [±45, 0/90], Core: Nomex honeycomb 8 mm, Width w = 100 mm, Length [350(180) mm]
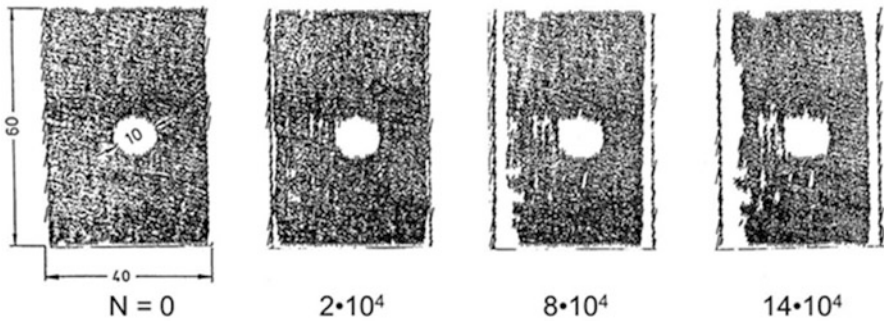
Fig. 3.47 Delamination growth under fatigue loading of a $[0_2, +45, 0_2, -45, 0, 90]_S$ laminate with an artificial delamination ∅10 mm in the middle, stress amplitude ±400 MPa, R = −1, the number of cycles until collapse N = $14{,}2{\cdot}10^4$

the panel was loaded almost by collapse load. One cycle took 7 s. The figure shows thermography images at different cycles until collapse. In the first figure, the artificial separation of the second stringer is visible. In the next steps, other stringers start to separate from the skin. But the artificial separation does not grow until collapse (Degenhardt et al. 2008).

Cycle 2801, u = 1.8 mm   Cycle 3201, u = 1.8 mm   Cycle 3601, u = 2.0 mm

Cycle 4001, u = 2.0 mm   Cycle 4016, u = 2.0 mm   Cycle 4017, u = Collapse
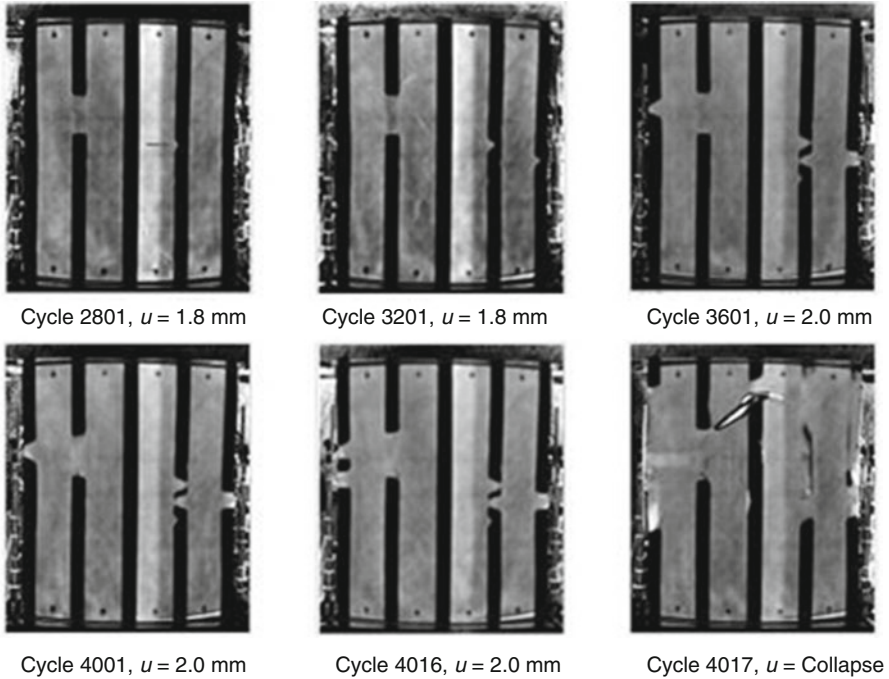
Fig. 3.48 Thermography images of a stiffened CFRP panel cyclically loaded by axial compression

3.3 Defects in Coatings

The main aim of the use of coatings (thin or thick films) in aircraft structures is to reduce or delay the effect of corrosion and wear in the component's structural integrity. These are important as corrosion and wear can cause serious safety and economic effects in the aerospace sector. Coatings of aircraft structures are expected to have a prolonged life in a very demanding or extreme environment, which includes thermo-mechanical loading cycles and ultraviolet radiation (Tiong and Clark 2010). The intrinsic resistance of the underlying substrate (alloys) alone is not sufficient to protect aircraft structural surface from demanding or extreme environments (Tiong and Clark 2010). Combination of corrosion and wear remain some of the considerable risks to aircraft structures and their integrity; both can decrease substrate section thicknesses, initiate micro-cracks, create stress concentrations zones and potentially inducing fatigue cracking leading to catastrophic failure. High quality coating material requirements for aeronautical applications makes the defect detection and inspection techniques of prime importance, both in manufacturing and in-service operation. The following subsections describe the major defects encountered in coating materials.
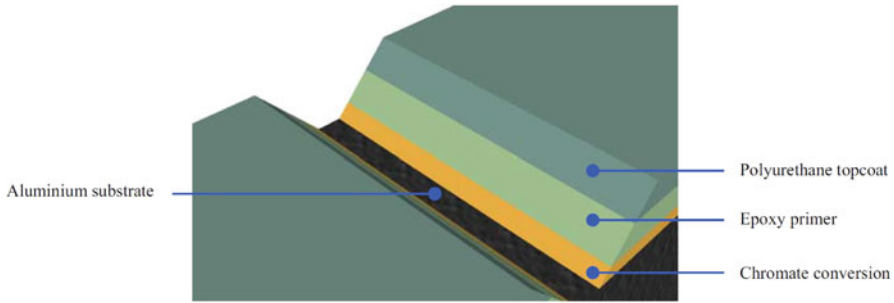
Fig. 3.49 Aircraft structural coating that consists of polyurethane topcoat, epoxy primer, chromatic conversion on the aluminium substrate (Tiong and Clark 2010)

### 3.3.1 Defects During the Manufacturing Process

One of the main aspects of applying surface coatings to the substrate is to improve the overall performance of the coated components. This can be achieved through the proper application of coatings technology, their characterization, testing and evaluation. As an example (Fig. 3.49), for corrosion-resistant applications, most aircraft surfaces are painted with a shielding layer consisting of chromatic conversion on the substrate, an epoxy primer and a polyurethane topcoat (typical total thickness of about 50–125μm). The role of epoxy primers is to inhibit corrosion of underlying substrates, whereas the topcoat (polyurethane) is a layer that is resistant to a range of chemicals and weather, largely flexible layer and provides the desired surface appearance. A layer of sealant coat is useful at faying surfaces (surfaces that are in contact at a joint) to help provide the flexibility of the layer and prevent cracking (Tiong and Clark 2010).

Some of the manufacturing defects in paint layer during the application, drying and curing stages may include bleeding (leeching out of the painted layer), sagging (dripping of paint from top to bottom forming wavy appearance), wrinkling (formation of undulating wrinkling film), crawling (inability to form a film), crating (formation of small bowl-shaped depressions), lifting (by layers of coating on existing paint), prolonged drying time (inability to dry) and loss of gloss (caused by severe absorption of undercoat).

Beyond corrosion-resistant applications where paints are most suitable, over the last few decades, the number of coating of film deposition methods for wear protection in high-temperature applications such as chemical vapour deposition, physical vapour deposition, electrodepositing, radio frequency ion source implantation, electron beam implantation, thermally sprayed coating (air plasma, flame spray, high-velocity oxy-fuel), chemical catalytic reduction deposition, vacuum-diffused deposition and plasma arc deposition has evolved (Awang et al. 2020). There are many but some of the materials as a thin protective coating for aircraft applications are polymer, ceramic, diamond-like carbon (DLC), TiN, NiTi, (TiB+TiC)/Ti64, TiAlN, AlCrN, Al_2O_3, WS_2 and stellite.

Considering thermal spray coating technology in the aerospace and defence sector, it is used in a range of applications which includes landing gear parts (bearings, axles, pins), jet engine parts (blades, vanes, combustion liners, compressor casings, nozzles), actuation parts (pistons, pumps, flaps), engine cowling and wing span structures. Thermal spray coatings (e.g. using thermal barrier materials) protect engine turbine blades from high temperatures and ensures high reliability for a long period of time. In landing gear parts, thermally sprayed coatings are replacing hard chromium plating as the preferred coating method to provide improved mechanical performance. Some of the coating materials manufactured using thermal spray coating techniques are metals (e.g. MCrAlY), ceramics (e.g. zirconia, alumina), cermets (e.g. WC-Co) and composites (Gansert 2013).

Taking an example of alumina (Al_2O_3) coatings sprayed onto steel substrates using thermally sprayed techniques, have been used in aircraft parts because of their wear resistance properties (Thirumalaikumarasamy et al. 2014). Figures 3.50 and 3.51 shows some of the manufacturing features and defect in thermally sprayed coatings (air plasma spray-APS and high-velocity oxy-fuel-HVOF). The sprayed surfaces (Fig. 3.50a, b) show that the Al_2O_3 particles have spread and non-melted or semi-molten particles not distinguishable. Polished cross-sections of the sample (Fig. 3.50c, d) show a qualitatively higher porosity for the APS alumina
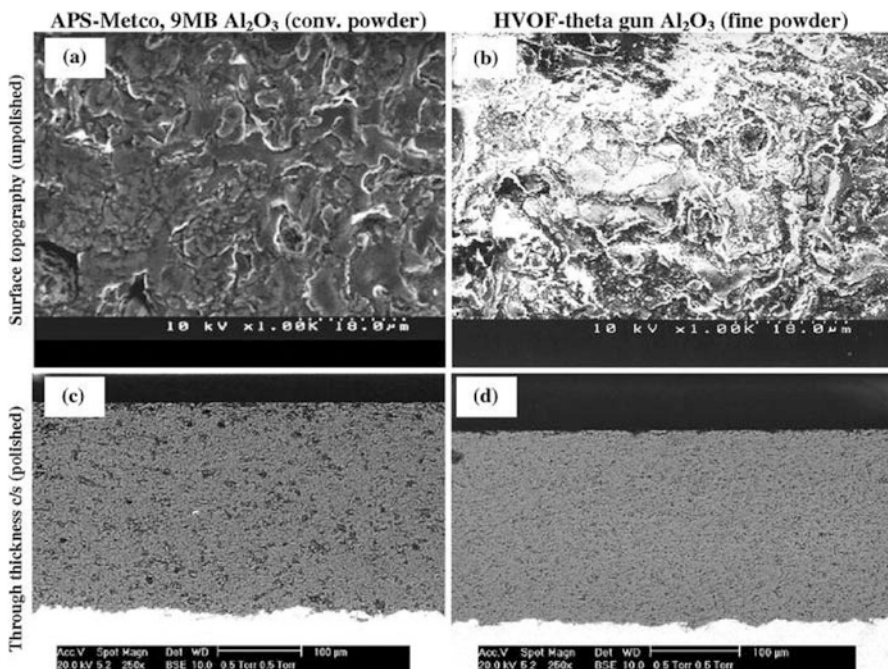
Fig. 3.50 Thermally sprayed alumina coatings on steel substrates: (**a**) and (**b**) showing surface topographies with definite splat morphologies, (**c**) and (**d**) through-thickness coating cross-sections (polished surface) (Ahmed et al. 2012)

(conventional powder) than HVOF alumina (fine powder). Average coating porosity was measured as 2.8% and 8.8% for the HVOF and APS coatings, respectively (Ahmed et al. 2012). The microscopic investigation revealed pores, voids, un-molten particle, non-bonded inter-splat areas and vertical cracks in splats, including columnar grain structure in lamellae (Fig. 3.51).
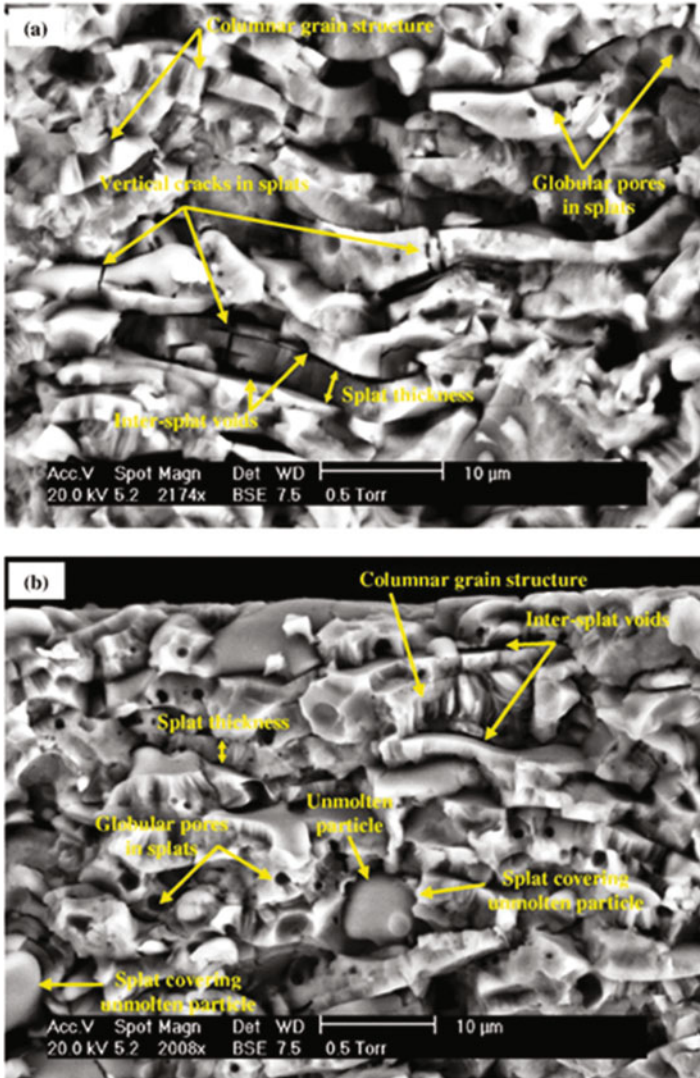
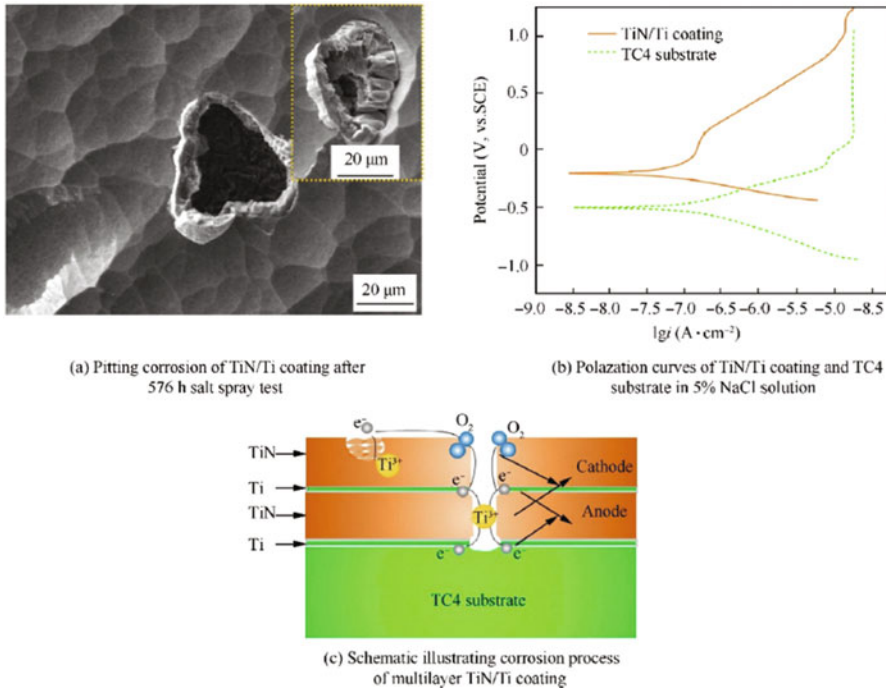**Fig. 3.51** SEM images of Al_2O_3 coatings (cryogenically fractured coating flakes) showing splat morphologies with columnar grain structure, pores, voids, vertical cracks in splats and unmolten particles: (**a**) APS Al_2O_3 and (**b**) HVOF Al_2O_3 (Ahmed et al. 2012)

All such coatings with underlying substrates require an optimized process parameter for coatings to adhere for a long period of time under service conditions. However, each of the coating deposition methods could induce some manufacturing defects if the process parameters are not appropriately managed. This can include poor adherence of coating to the substrate, high porosity, micro-cracks, non-uniform mechanical properties, through-thickness tensile residual stresses, poor wear resistance (sliding/erosive/abrasive), poor thermo-mechanical behaviour, etc. However, with the advancement in the coating deposition technologies and process optimization and control, it has been anticipated that the coating materials deposition quality measured during manufacturing is critical for enhancing our understanding of future generation applications (e.g. high-speed aircraft). Post-manufacturing coating characterization can include various microstructural characterizations and understanding the role of structure-property relationship through advanced characterisation tools (e.g. nanomechanical testing (Faisal et al. 2014; Faisal et al. 2017), acoustic emission sensor based in-situ mechanical testing (Faisal et al. 2011a), neutron diffraction residual strain testing (Ahmed et al. 2012), tribomechanical testing (Ali et al. 2017)). Overall, the coating tests can include mechanical, physical, chemical and weathering, whereas, the coating evaluation can include evaluation under various environmental conditions (e.g. under normal operation and/or in corrosive and wear conditions). All these testing including testing with sensors have the potential to improve our understanding of the structure-property relationships and failure characteristics of current and future generation coatings or thin films.

3.3.2   Defects During In-service Conditions

In-service defects in coatings can be classified according to the nature of environmental damage (corrosion, wear) and physical damage (thermo-mechanical loading) in aircraft structure. Overall, the testing of the integrity of coatings onto the substrate is extremely important for the evaluation of the coating-substrate system. Considering the extreme loading conditions in which the aircraft operates (more for the military than civilian aircraft), the obligation of very high mechanical strength of coating-substrate system deviates other gradual concerns (e.g. corrosion, wear) (Korb and Olson 1997). However, in all cases, it is important that coating is resistant to corrosion, has high adhesion strength with the substrate or between various layers and minimize creep in high-temperature conditions (Pokluda 2010).

Several coatings have been applied to aircraft engine parts (e.g. compressor blades) to develop multifunctional erosion and corrosion mitigations in harsh in-service conditions (Sun et al. 2020). In this work, the multi-arc ion plating technique was applied for TiN/Ti coating fabrication on the TC4 (Ti-5.60Al-3.07V, wt%) substrate. Note that such nitride coating depends not only on high mechanical strength but also on the complex mix of environmental conditions such as erosion and corrosion. Figure 3.52 shows the morphology and mechanism of pitting corrosion of TiN/Ti coating onto TC4 after 576 h salt spray corrosion). From

(a) Pitting corrosion of TiN/Ti coating after 576 h salt spray test

(b) Polazation curves of TiN/Ti coating and TC4 substrate in 5% NaCl solution

(c) Schematic illustrating corrosion process of multilayer TiN/Ti coating

Fig. 3.52 Morphology and mechanism of pitting corrosion of TiN/Ti coating (Sun et al. 2020)

the Tafel polarization plots in Fig. 3.52b, it was observed that the corrosion potential difference promoted the corrosion cells between TiN and Ti, which were the cathode and anode for electrochemical corrosion (Sun et al. 2020), respectively, with corrosion process schematic shown in Fig. 3.52c. It was concluded that the structural design of multilayer dense coatings can be an improved way to prevent the medium of corrosion solutions.

Common defects in paint coatings during service life could be peeling or flaking, chalking, blistering, rust staining, algae or fungi growth, etc. For each of these defects, it requires a range of preventive and remedial methods that are necessary to rectify any unexpected defect.

Wear or damage of the coated surface due to the impact of small sand particles or large objects (such as bird strike), including indentation of the structure during handling process is what is thought to be the most common reason of inducing surface defects. If the coating layer is brittle, then potentially failure such as peeling or flaking can occur (e.g. Fig. 3.53). Physical damage to the coated surface can include thermal shock and fatigue while operating at various altitudes.

In most cases, the coating and substrate materials have different thermal expansion properties, therefore, a combination of thermal shock and fatigue loading can induce coating failure. During in-service conditions, as an example, the engine does not run constantly; therefore, during every flight, a change in thermo-mechanical
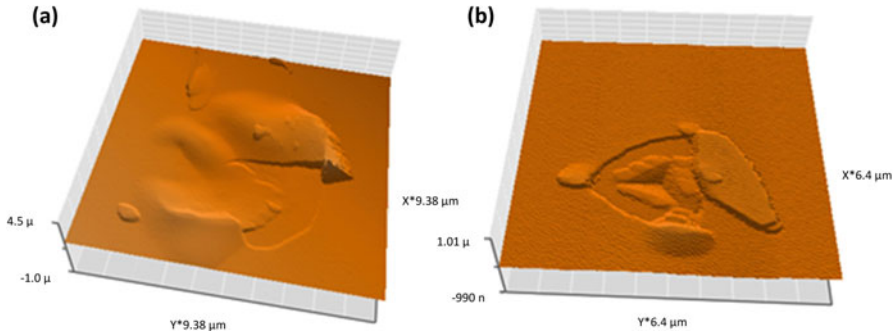
Fig. 3.53 Failure in brittle coating (100 nm thick DLC on silicon substrate) during 20-cycles nanoindentation: (**a**) under conical indenter at 200 mN and (**b**) Berkovich indenter at 10 mN

loading will cause significant strain mismatch at the interface of the coating-substrate system, leading to thermal fatigue damage to the coatings mainly.

The ductile-to-brittle transition (DBT) is important for the understanding of fracture or failure processes (Milne et al. 2003). In aircraft engine parts with coatings, if the ductile-to-brittle transition temperature of coatings is within the temperature range of the engine start phase, then the thermo-mechanical loading stress can cause failure in coatings. As the aircraft flies in airspace with various moisture contents and potentially a corrosive environment with excessive temperature would have an add on effect (oxidation and reduction of materials) to those effects mentioned above, leading to coating failure.

Coated components in aircraft structures when properly tested and in-situ monitored using sensors during in-service operations, can ensure a satisfactory lifespan before being further used. It is understood that regular maintenance may reduce the occurrence of in-service failures in coatings and associated parts by replacing suspect parts. However with the nature of some of the aircraft parts (e.g. turbine engine, landing gear), it is difficult all the time to inspect thoroughly each element of a given assembly. As such the structural health monitoring (SHM) using advanced sensing tools may be a way forward.
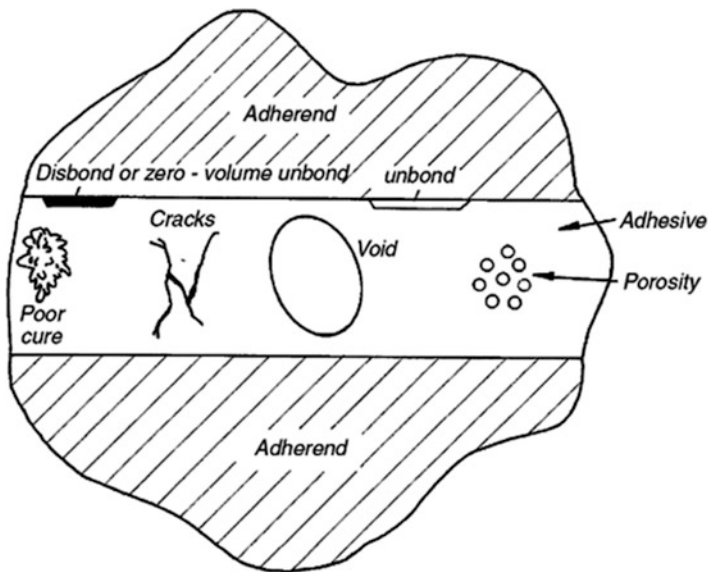
3.4 Defects in Joints

3.4.1 Adhesively Bonded Joints

Adhesive bonding of primary aircraft structures has been in use for more than 60 years. The qualification process of new adhesive technology is a protracted process involving fluid immersion testing, high, low and cyclic thermal performance testing followed by static buckling and fatigue testing. Adhesive bonding is for

example used in bonding stringers to the fuselage and to the skin to stiffen the structures against buckling. It is also used to manufacture the honeycomb structures used in the flight control structures such as elevators, ailerons, spoilers etc. Defects can be introduced both in manufacturing and during service. Thus, the characterization of defects both at the manufacturing and during service conditions is important. The qualification of an adhesive system is carried out not to assess the static performance but to evaluate the long-term durability. The evaluation is usually in comparison with an existing proven technology.

The aim of defect identification and characterization in adhesive bonds is to understand the mechanisms that lead to the creation of the defect, the effect of the defect on the performance of the adhesive joint and ultimately the damage tolerance of the joint. As with fastener-based joints, where the repair can be performed and the joint performance reinstated to 100% post-repair through a simple replacement of the fastener, a 100% regain of the adhesive joint strength is impossible unless a complete reapplication of the adhesive is performed. Hence, the defect type (e.g. Fig. 3.54) and severity must be identified accurately to assess the residual strength of the adhesive bond.

The adhesive bonding of two substrates is a complex phenomenon involving various fields of study. Several theories have been proposed to explain the bond formation, some of them being, mechanical interlocking, interface layer formation, weak boundary layer formation etc. The defects observed in adhesive bonds can be broadly classified into two categories namely those created during the manufacture and in-service defects. Manufacturing defects are created due to improper fabrication

**Fig. 3.54** Defects in an adhesive bond (da Silva et al. 2018)

Fig. 3.55 Void in the adhesive caused by premature handling of the joint before the adhesive cured (da Silva et al. 2018)

techniques related to substrate preparation and adhesive application. Conversely, service defects can be created due to environmental and operational loading factors.

Manufacturing defects in adhesive bonds are classified into three main types: (a) complete voids, disbonds, porosity. This type of defect occurs because of air trapped within the adhesive during the fabrication stage (e.g. Fig. 3.55), the presence of volatiles, defects in the application of the adhesive or insufficient quantity of adhesive. The mixing of the adhesive and hardener during fabrication can sometimes introduce air trapped within the mixture (b) poor adhesion, the improper bond between the adherends and the adhesives. This kind of defects occurs due to improper surface preparation and impurities being present on the surfaces of the adherends before fabrication and (c) kissing defects caused by the local disbonding of the adhesives and adherends. These are also called zero volume disbonds due to the very small dimensions along with the thickness. The wider category of surface disbonds into which kissing bonds fall into that created by the application of adhesive only on one of the adherends in the fabrication stage. Kissing bonds are the worst case of this.

The definition of kissing bonds varies, and several conflicting statements have been made in the literature. For example, Nagy (1991) defined kissing bonds as contact between two compressed but otherwise unbonded surfaces. Jiao and Rose (1991) defined them as two surfaces in perfect contact with each other, however without any ability to transmit shear stresses. However, this definition is not valid in the case of real adhesive bonds as no two surfaces can be in perfect contact and so can be applied in modelling studies only. They also proposed another method of modelling the joint with a thin layer of liquid present between the two disbonded
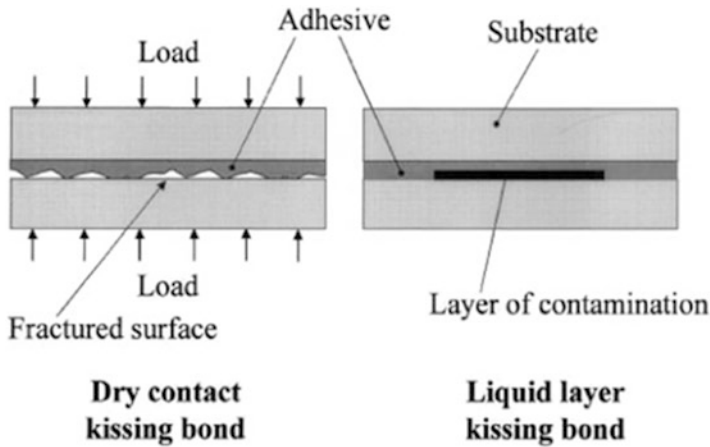
Fig. 3.56 Schematics of dry contact and liquid layer kissing bonds (Brotherhood et al. 2002)

surfaces. Due to the intimate contact of the surfaces in a kissing bond (e.g. Fig. 3.56), where some or all of the surface asperities on both the surfaces are in contact, despite the complete lack of adhesive strength, they are very difficult to detect with many of the conventional non-destructive evaluation techniques. With this combination of undetectability and severity, the presence and detection of kissing bonds present a significant practical problem in the application of adhesive bonds in primary load-carrying structures.

Problems with curing in terms of temperature, cure time or the improper mixing of the different parts of the adhesive mixture also cause porosity and adhesive cracks within the adhesive layer. Poor cure sometimes adjusts itself as the adhesive cures, though slowly. Voids are sometimes also caused because of the relative motion of the adherends with respect to each other during the cure (Fig. 3.55). The presence of voids has been shown to not have a significant effect on the failure initiation in lap joints (Karachalios et al. 2013). This was because, in most of the joints, the failure strain of the adhesive is quite low compared to the yield strength of the adherend materials used. However, if a rubber toughened epoxy were to be used along with high strength alloys for the adherends, the joint strength is almost proportional to the bonded area (Karachalios et al. 2013).

A brief discussion on the effect of the external contaminants introduced in the fabrication stage is given in the following paragraphs. Surface contaminants can be broadly categorized into two groups, namely organic and inorganic. The surface preparation required before bonding is different in each case, organic contaminants being the easier to remove through a simple degreasing process. Inorganic contaminants, conversely, need to be removed by degreasing, de-smutting and in some cases, deoxidization. Surface contamination tends to reduce the surface free energy. The effect of surface contaminants is studied by Smith and Crane (1980) using different levels of the controlled introduction of contaminants on the adherend surfaces. Contaminants like silicone grease, oils, fingerprints, cigarette smoke

residues, mucous, drink residues, lubricating oil were introduced on aluminium adherends which were chromium acid and phosphoric acid anodized. In joints with lubricating oil introduced, no significant reduction in the lap shear strength has been observed at contaminant thicknesses of 10 nm. However, in the case of silicone grease, a significant reduction in strength was observed in the contaminant thickness range of 3.5–20 nm. This is accompanied by a tendency towards a dominant interfacial failure. In the automotive industry, tolerance of adhesive bond strength to surface contamination of adherends has been tested. For example, Minford (1981) evaluated the effect of adherend immersion in lubricant solution on the joint strength. He reported that the presence of the oil did not make any difference till the surface concentration reached 0.95mg/cm^2. The strength of the bond dropped by around 50% and the failure transitioned from 90% cohesive to more than 40% interfacial adhesive failure. Similarly, the bonds retained their original strength till an oil concentration of 0.62 gm/cm^2 when exposed to a humid or salt spray environment for 180 days. The effect of the presence of oil has been found to reduce the glass transition temperature (T_G) during the cross-linking process while curing. This has been noticed with an adhesive containing 6% dicyandiamide and with the same adhesive containing $CaCO_3$ filler. The reduction in TG was not noticed in the case of fully cross-linked adhesive. Similarly, Anderson (1993) studied the effects of HD-2 grease contamination on one of the adherends on the double tapered cantilever beam and butt joint tensile test performance. Hysol EA913 and EA946 were tested and the former exhibited a 50% reduction in the tensile strength at an oil contamination of 400 mg/m^2, whereas the latter did not exhibit any reduction in strength.

Interfacial degradation appears in adhesive bonds when exposed to environmental factors such as high temperature and humidity. The bond formation across the interface is due to secondary and dispersive forces across. The interface work of adhesion is found to be a function of the interfacial free energies of the adherend and adhesive and the surface free energy. Metals tend to form oxide layers on the surface which are polar. This polar nature attracts water molecules which themselves are polar because of the hydrogen bonds. This leads to a disruption in the interfacial bonding between the adhesives and adherends. The work of adhesion in an inert environment tends to be positive leading to a strong bond, whereas in the presence of moisture, the work of adhesion could be negative leading to a disbond along the interface. In addition, certain metal oxides, such as aluminium oxide, react with water to form hydroxides which exhibit loose adhesion to the metal surface leading to a weak interfacial layer.

The general effect of hot and humid environments on the adhesive bond strength is summarised in Fig. 3.57. It shows the aluminium alloy lap joint strength degradation with respect to time of exposure to humidity. As shown, lower levels of humidity have significantly less effect on the bond strength compared to higher levels. This leads to the argument that there exists a critical concentration of moisture in the adhesive below, in which there will be no joint strength degradation. The dotted line in the plot indicated the strength recovery in a joint exposed to high humidity levels after exposure to lower humidity levels. This was attributed to the
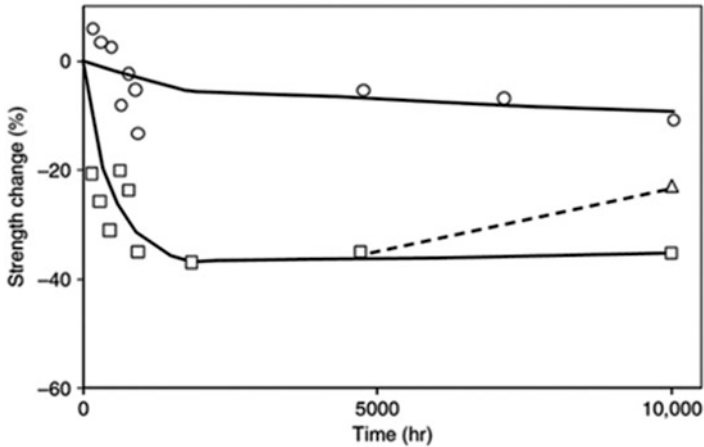
Fig. 3.57 Nitrile-phenolic adhesive-bonded aluminium alloy joints exposed to wet air at 50°C and circle legend—50%RH, square legend—100%RH, triangle legend—joint exposed to 100%RH for 5000 h and stored at 50% RH for 5000 h (Comyn et al. 1987)

failure in the primer close to the oxide layer rather than directly at the interface. The effect of moisture diffusion into the adhesive cannot be reversed and the joint strength degradation is irreversible. Moisture ingress in adhesive bonds can either be through direct absorption and diffusion through the adherends and the adhesive. In some cases, where the adherend diffusion is not possible, the cracks and voids present within the bond line promote the moisture uptake. Moisture usually leads to plasticization of the adhesive and/or changes in the glass transition (T_G) temperature in some cases. The rate at which the moisture diffuses into the bond line depends on the diffusion coefficient which in turn depends on the environmental temperature. Hence, hot and wet environments pose the most aggressive form of accelerated ageing to adhesive bonds.

Moisture diffusion in adhesives is dictated by Fick's law where the rate of diffusion of water is directly proportional to the square root of the exposure time. Where case II diffusion dynamics are in play, the diffusion rate is directly proportional to the exposure time. This is characterized by a saturated and swollen diffusion front travelling through the pristine polymer. Though Fick diffusion is seen in most adhesives, environmental conditions such as high temperature and high humidity tend to promote case II diffusion. Evidence has also been recorded of bulk adhesives that exhibit Fickian diffusion behaviour exhibit case II diffusion when bonded in a joint (Liljedahl et al. 2009). Once diffusion occurs, the moisture either occupies the free spaces or voids within the bond line as free water or exists as bound water. Bound water is responsible for the volumetric changes within the bond line, leading to residual stresses and undesirable stress concentrations which further promotes case II diffusion (Adamson 1980). The bound water can further be classified into Type I and Type II, in which Type I is responsible for single hydrogen bonds that

result in plasticization of the adhesive and reduction in the TG value of the adhesive (Zhou and Lucas 1995; Zhou and Lucas 1999a). Type II is where the water molecules form multiple hydrogen bonds lead to a promotion in secondary cross-linking and thus do not have a significant effect on T_G as that of Type I (Zhou and Lucas 1995). Typically, Type I water can be removed by low-temperature heating, Type II might need heating to a higher temperature (Zhou and Lucas 1999b). Kinloch et al. (2000) have reported that relatively viscous adhesives have difficulty penetrating the asperities and pores within the adherend and so promote the diffusion of moisture along the interface leading to premature rupture of the joint. However, when a low viscosity primer was applied to the adherend before adhesive application, the strength reduction has decreased drastically as the primer fills in the gaps which could be occupied by water. Similarly, moisture absorption in composite pre-pregs before curing is known to cause significant problems in bonding. The absorbed moisture diffuses to the surface of the substrate upon curing thus completely preventing any adhesion along the interface.

3.4.2   Friction Stir-Welded Joints

Metallic materials can be joined by a variety of methods including welding, brazing, adhesive bonding and mechanical fastening. For aerospace applications, friction stir welding (FSW) is very attractive because of ability to weld butt, lap- and T-joints, the ability to join difficult to weld classical alloys, ability to join dissimilar alloys, possible elimination of cracking in the fusion and heat-affected zone (HAZ), lack of weld porosity, etc. (Campbell 2006; Myśliwiec and Śliwa 2018; Śliwa et al. 2019; Myśliwiec et al. 2019).

Friction stir welding (FSW) is a solid-state joining process. It involves rotating a cylindrical tool with a short protrusion or 'pin', which is plunged between two metal plates (Fig. 3.58).

High pressure and shear strain plastically deform and consolidate the workpieces using material extrusion from the front to the back of the tool. The plates are clamped with a sturdy fixture to the backing plate with an anvil piece of hardened steel
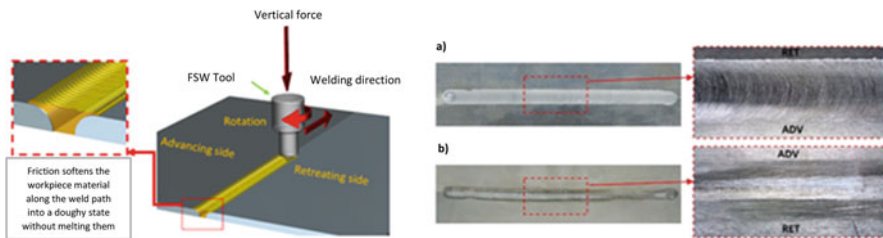

Fig. 3.58 Scheme of the FSW process—a lap joint and example joint without any defect (advancing side-**a**, retreating side-**b**) (Myśliwiec et al. 2019)

underneath the path of the FSW tool, counteracting the vertical and horizontal forces arising during welding. The combination of frictional and deformation heating around the immersed rotating pin and at the interface between the shoulder of the tool and the plates leads to the consolidation of the two metal plates as the tool traverses along the joint line. FSW process was invented in the Welding Institute (TWI) in the UK in 1991 and has been researched extensively since then and applied in various fields such as the automotive, marine and aerospace industries, where aluminium alloys are heavily used (Thomas et al. 1991; Huang et al. 2018).

Global trends in CO_2 emission and gas price have attracted extensive attention from the automotive manufacturing industry to produce lighter, safer and environmentally friendly vehicles (Guo et al. 2019). In conventional FSW, a tool consisting of a probe and a shoulder was commonly used. Generally, the diameter of the shoulder is about three times bigger than that of the probe. However, this type of tool is associated with several issues. One is the significant through-thickness temperature gradient because the heat generated by the shoulder is much higher than that by the probe, with the peak temperature developing at the top surface, which affects joint microstructure and properties. Another issue is the generation of the flash and arc corrugation because some plastic material moves out of the weld (Zhang et al. 2012).

To receive good welds of metals using friction stir welding (FSW) and avoid defects of such joints it is necessary to know characteristics of the material flow of alloys in FSW (e.g. Colligan 1999) by using a tracer material. Xu et al. (2001) developed two finite element models to predict the material flow during the FSW of Al alloys. Mishra and Ma (2005) described the current state of understanding and development of FSW. Fujii et al. (2006) demonstrated the influence of tool geometry, welding parameters and joint configurations on material flow and temperature distribution in FSW. Vijayan and Raju (2008) outlined the detailed parameters governing the joining process, including the rotation rate, welding speed, axial force and tool geometry. Kulkarni et al. (2018) investigated the influence of the type of the backing plate material on weld quality. Hook defects on AS (advancing side) and on RS (retreating side) of SSFSLW (stationary shoulder friction stir lap welding) joints at different welding speeds have been identified by Wen et al. (2019).

The FSW weld does not demonstrate many of the defect encountered in normal fusion welding and distortion is significantly less. But to consider the influence of all conditions and the process parameters on the final result of joining, it could be shown that the main possible defects (e.g. Fig. 3.59) occur when there is an inappropriate choice of parameters for a given case, especially for welding very thin sheets, and when plastic flow and stir materials in the welding zone are difficult to realize. The welds are created by the combined action of frictional heating and plastic deformation of the joined materials due to the rotating tool. To avoid defects, all important parameters, mainly the speeds and feeds influencing the heat input during welding, must be carefully chosen.
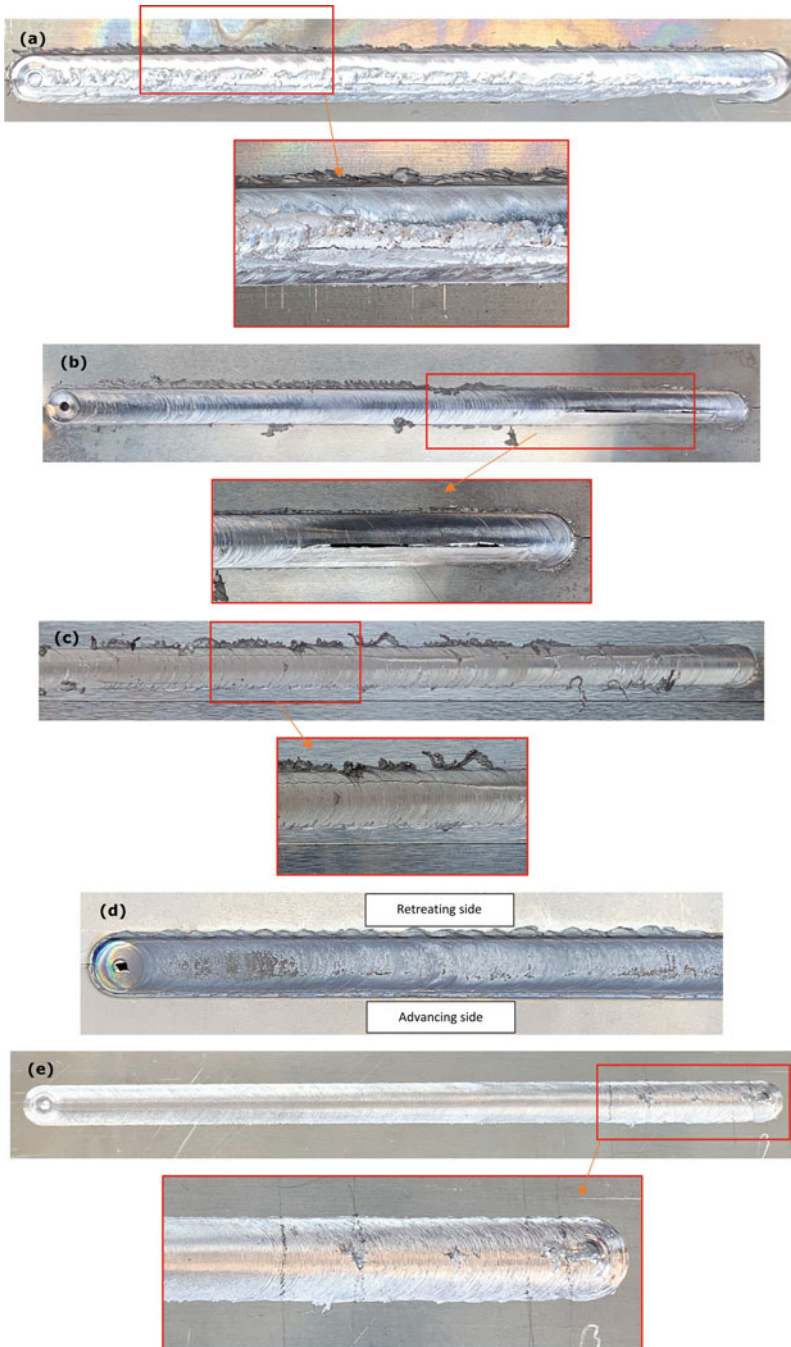
Fig. 3.59 Friction stir weld (FSW) joints with defects; (**a**) butt joints of AA2024-T3 of 2 mm in thickness defect types: exceeds flash, cracking of the joints, the unnormal stirring of the material, (**b**) butt joints of AA7075-T6 of 0.5 mm in thickness, defect types: exceeds flash, wormhole, (**c**) lap joints of AA2024-T3 1 mm in thickness, defect types: exceeds flash, cracking of the joints, (**d**) butt joints of titanium grade 5 of 0.5 mm in thickness, defect types: excessive oxidation of the joints and (**e**) butt joints of AA2024-T3 of 0.5 mm in thickness, defect type: cavities

3.5   Concluding Remarks

Understanding the fundamental nature of material defects or imperfections during manufacturing and in-service condition has been very important in materials and structural design of aircrafts over the last decades. Apart from testing and characterization of materials and structures using standard procedures, the application of sensors to carryout destructive, semi-destructive or non-destructive testing techniques are useful tools for investigating the condition of the materials or structural parts.

In the following chapters, the state-of-the-art methods of SHM and damage detection systems have been clearly laid out. Over the last years, the advancement in sensors, instrumentation, signal and image processing, including statistical analysis techniques, has led to a rapid change towards digitization (i.e. conversion to digital format) and digitalization (i.e. the use of digital technologies) of various sectors, including those in materials and manufacturing. Application of principles of artificial intelligence (AI) and machine learning (ML) approaches for digitalization is likely to bring substantial improvements in operational efficiency, defect detection, decision making and materials cost efficiency of aircraft structures.

If the structure of an aircraft is monitored, a tremendous amount of data can be generated by everyday operations. While there are existing methods of SHM and damage detection systems, but not clear how much is of current interest. Therefore, it is necessary to develop new improved models based on data-driven as well as theory-driven methodologies in real operation of aircraft and check the validity of existing models by synthesizing prior knowledge along with multimodal data in machine learning approaches.

Potentially, the systematic creation of digital twin (DT) to understand the fundamental nature of material defects or imperfections during manufacturing and defect during the in-service condition in aircraft structures can be a way forward. Through this, the utilization of large sets of Internet of Things (IoT) sensors data and combining it with historical findings in physical modelling along with artificial intelligence and advanced statistical algorithms can help in providing a near-real-time representation of aircraft structural defect analysis. With such a method, a continuous SHM monitoring and defect inspection can be done to save the efforts by physically inspecting the real aircraft asset. Also, it can be used for the pattern of aircraft structure manufacturing analysis, structural parts life estimation, failure diagnostics and prognostics, structural integrity monitoring and long-term production estimation. All such advancement can help in developing an intelligent decision support system for the type of defect in the various structural materials or parts.

References

Abrate S (1991) Matrix cracking in laminated composites: a review. Compos Eng 1:337–353. https://doi.org/10.1016/0961-9526(91)90039-U

Adamson MJ (1980) Thermal-expansion and swelling of cured epoxy-resin used in graphite-epoxy composite- materials. J Mater Sci 151736-1745. https://doi.org/10.1007/BF00550593

Aeronautics Guide, Forms of Corrosion (2019) Aircraft corrosion control, https://www.aircraftsystemstech.com/2019/04/forms-of-corrosion-aircraft-corrosion.html

Ahmed R, Faisal NH, Paradowska AM et al (2012) Residual strain and fracture response of Al_2O_3 coatings deposited via APS and HVOF techniques. J Therm Spray Technol 21:23–40. https://doi.org/10.1007/s11666-011-9680-7

Aircraft Owners and Pilots Association (n.d.) Aircraft Corrosion, Aircraft Owners and Pilots Association Website, https://www.aopa.org/go-fly/aircraft-and-ownership/maintenance-and-inspections/aircraft-corrosion

Alemour B, Badran O, Hassan MR (2019) A review of using conductive composite materials in solving lightening strike and ice accumulation problems in aviation. JAerosp Technol Manag 11:e1919. https://doi.org/10.5028/jatm.v11.1022

Ali O, Ahmed R, Faisal NH et al. (2017) Influence of post-treatment on the microstructural and tribomechanical properties of suspension thermally sprayed WC–12 wt%Co nanocomposite coatings. Tribol Lett 65:33. doi:https://doi.org/10.1007/s11249-017-0815-y

Al-Jabbouli H, Koç E, Akça Y (2015) Classification of main faults in the production process of extruded aluminium profiles. Int J Eng Technol 7:84–90

Anderson GL (1993) Continuum and fracture mechanical studies of contaminated bonding surfaces. J Adhes 41:129–137. https://doi.org/10.1080/00218469308026558

Antonucci V, Cusano A, Giordano M et al. (2006) Cure-induced residual strain build-up in a thermoset resin. Compos A 37:592-601. doi:https://doi.org/10.1016/j.compositesa.2005.05.016

Archer E, McIlhagger A (2015) Ch. 14 repair of damaged aerospace composite structures. In: Soutis C (ed) Polymer composites in the aerospace industry. Woodhead Publishing, Irving PE, pp 393–412

Arrieta AJ, Striz AG (2005) Optimal design of aircraft structures with damage tolerance requirements. Struct Multidisc Optim 30:155–163

Awang M, Khalili AA, Pedapati SR (2020) A review: thin protective coating for wear protection in high-temperature application. Metals 10:42. https://doi.org/10.3390/met10010042

Banis D, Marceau JA, Mohaghegh M (1999) Design for corrosion. Aero Magazine, Issue 7, July 1999, Boeing. Available also, http://www.boeing.com/commercial/aeromagazine/aero_07/corrosn.html

Bhadeshia HKDH (2006) Aircraft undercarriage: martensitic steel. https://www.phase-trans.msm.cam.ac.uk/2006/Undercarriage/Undercarriage.html

Black S (2013) Lightning strike protection strategies for composite aircraft. Composite World. https://www.compositesworld.com/articles/lightning-strike-protection-strategies-for-composite-aircraft

Blaha J, Krempaszky C, Werner EA (2002) Carbide distribution effects in cold work tool steel. Proceedings of the 6th international tooling conference. Karlstad University, Karlstad, pp 289–298

Bolotin VV (1996) Delaminations in composite structures: its origin, buckling, growth and stability. Compos Part B 27:129–145

Brand C, Boller C (1999) Identification of life cycle cost reduction in structures with self-diagnostic devices. NATO RTO symposium on design for low cost operation and support. Ottawa, Canada, 21–22 October 1999.

Brooks CR, Choudhury A (2002) Failure analysis of engineering materials. The McGraw-Hill Education, New York, NY. http://www.ncbi.nlm.nih.gov/pubmed/101221

Brotherhood C, Drinkwater B, Guild F (2002) The effect of compressive loading on the ultrasonic detectability of kissing bonds in adhesive joints. J Nondestruct Eval 21(3):95–104

Campbell FC (2006) Manufacturing technology for aerospace structural materials. Elsevier, Amsterdam

Civil Aeronautics Board, Accident Investigation (1949) Available report, SA-178, File No. 1, https://www.baaa-acro.com/sites/default/files/import/uploads/2016/04/NC93044.pdf. Released 0117

Colligan BK (1999) Supplement to the Weld J 6:229–237

Comyn J, Brewis DM, Tredwell ST (1987) Bonding of aluminium alloy with some phenolic adhesives and a modified epoxide adhesive, and strength changes on exposure to moist air at 50°C. J Adhes 21(59-78):59–78. https://doi.org/10.1080/00218468708074959

Criou O (2007) A350 XWB family & technologies. Presentation at Hamburg University of Applied Sciences 20 September 2007. https://www.fzt.haw-hamburg.de/pers/Scholz/dglr/hh/text_2007_09_20_A350XWB.pdf

da Silva LFM, Öchsner A, Adams RD (2018) De/Anti-icing process coordination handbook of adhesion technology, 2nd edn. Springer International Publishing. https://deicing.net/

Degenhardt R, Wilckens D, Klein H et al (2008) Experiments to detect the damage progress of axially compressed CFRP panels under cyclic loading. Key Eng Mater 383:1–24

Dolbeer RA, Wright SE (2008). Wildlife strikes to civil aircraft in the United States 1990–2007. US Department of Transportation, Federal Aviation Administration, Office of Airport Safety and Standards, Serial Report 14. Washington D.C., USA

Dolbeer RA, Begier MJ, Miller PR et al (2019) Wildlife strikes to civil aircraft in the United States 1990–2018. US Department of Transportation, Federal Aviation Administration, Office of Airport Safety and Standards, serial report. Washington, DC, p 25

Ejaz N, Qureshi IN, Rizvi SA (2011) Creep failure of low pressure turbine blade of an aircraft engine. Eng Fail Anal 18:1407–1414. https://doi.org/10.1016/j.engfailanal.2011.03.010

Faisal NH, Ahmed R, Reuben RL (2011a) Indentation testing and its acoustic emission response: applications and emerging trends. Int Mater Rev 56:98–142. https://doi.org/10.1179/1743280410Y.0000000004

Faisal NH, Reuben RL, Ahmed R (2011b) An improved measurement of Vickers indentation behaviour through enhanced instrumentation. Meas Sci Technol 22:18 pp. art no. 015703. https://doi.org/10.1088/0957-0233/22/1/015703

Faisal NH, Ahmed R, Goel S et al (2014) Influence of test methodology and probe geometry on nanoscale fatigue mechanisms of diamond-like carbon thin film. Surf Coat Technol 242:42–53

Faisal NH, Prathuru AK, Goel S et al. (2017) Cyclic nanoindentation and nano-impact fatigue mechanisms of functionally graded TiN/TiNi film (Special edition on Functional Performance of Shape Memory Alloys). Shape Memory Superelasticity 3(2):149–167. https://doi.org/10.1007/s40830-017-0099-y

Fang T-T (2018) Point defects in crystalline materials. Elements of structures and defects of crystalline materials. pp 83–127

Findlay SJ, Harrison ND (2002) Why aircraft fail. Mat Today 5:18–25. https://doi.org/10.1016/S1369-7021(02)01138-0

Freitas M, Infante V, Baptista R (2019) Failure analysis of the nose landing gear axle of an aircraft. Eng Fail Anal 101:113–120. https://doi.org/10.1016/j.engfailanal.2019.03.010

Fujii H, Cui L, Maeda M et al (2006) Effect of tool shape on mechanical properties and microstructure of friction stir welded aluminum alloys. Mater Sci Eng A 419:25–31. https://doi.org/10.1016/j.msea.2005.11.045

Gädke M (1988) Hygrothermomechanisches Verhalten kohlenstofffaserverstärkter Epoxidharze. VDI-Bericht, Reihe 5, Nr. 136, VDI-Verlag, Düsseldorf

Gansert R (2013) Thermal spray coatings in the aerospace and defense industries. Int Thermal Spray Surface Eng 8

Gayathri P, Umesh K, Ganguli R (2010) Effect of matrix cracking and material uncertainty of composite plates. Reliab Eng Syst Saf 95:716–728. https://doi.org/10.1016/j.ress.2010.02.004

Gilbert JL (2020) Metals: basic principles, biomaterials science, 4th edn. pp 205–228.e1

Girodin G, Manes L, Moraux J-Y et al. (2002) Characterisation of the XD15N high nitrogen martensitic stainless steel for aerospace bearings. 4th International conference on launcher technology 'Space Launcher Liquid Propulsion', 3–6 2002. Liege, Belgium

Guo S, Shah L, Ranjan R et al (2019) Effect of quality control parameter variations on the fatigue performance of aluminum friction stir welded joints. Int J Fatigue 118:150–161. https://doi.org/10.1016/j.ijfatigue.2018.09.004

Hartman N (2008) Deicing an aircraft during a snow event. https://www.wikiwand.com/en/Deicing_fluid

Heimbs S (2012) Energy absorption in aircraft structures, In: International workshop on hydraulic equipment and support systems for mining, Huludao, China, pp 17-18

Hiroshi N (2014) Defects in metals, physical metallurgy, 5th edn. pp 561–637

Hu HW (2007) Physical aging in long term creep of polymeric composite laminates. J Mech 23:245–252. https://doi.org/10.1017/S1727719100001283

Huang Y, Wan L, Meng X et al (2018) Probe shape design for eliminating the defects of friction stir lap welded dissimilar materials. J Manuf Process 35:420–427. https://doi.org/10.1016/j.jmapro.2018.08.026

Jiao D, Rose JL (1991) An ultrasonic interface layer model for bond evaluation. J Adhes Sci Technol 5:631–646. https://doi.org/10.1163/156856191X00530

Karachalios EF, Adams RD, da Silva LFM (2013) Strength of single lap joints with artificial defects. Int J Adhes Adhes 45:69–76. https://doi.org/10.1016/j.ijadhadh.2013.04.009

Kinloch AJ, Little MSG, Watts JF (2000) The role of the interphase in the environmental failure of adhesive joints. Acta Mater 48:4543–4553. https://doi.org/10.1016/S1359-6454(00)00240-8

Korb LJ, Olson DL (eds.) (1997) ASM handbook – corrosion, 9th edn. ASM International 13

Kugler D, Moon TJ (2002) Identification of the most significant processing parameters on the development of fibre waviness in thin laminates. J Compos Mater 36:1451–1479. https://doi.org/10.1177/0021998302036012575

Kulkarni BS, Pankade SB, Andhale SR et al (2018) Effect of backing plate material diffusivity on microstructure, mechanical properties of friction stir welded joints: a review. Procedia Manuf 20:59–64. https://doi.org/10.1016/j.promfg.2018.02.008

Kutyinov VF, Ionov AA (1996) Ch. 1 specific features of composite-material structural design. In: Zagainov GI, Lozinolozinsky GE (eds) Composite materials in aerospace design. Chapman and Hall, ISBN 0412584700. pp 1–117

Lee BW, Suh J, Lee H et al (2011) Investigations on fretting fatigue in aircraft engine compressor blade. Eng Fail Anal 18:1900–1908. https://doi.org/10.1016/j.engfailanal.2011.07.021

Liljedahl CDM, Crocombe AD, Gauntlett FE et al (2009) Characterising moisture ingress in adhesively bonded joints using nuclear reaction analysis. Int J Adhes Adhes 29:356–360. https://doi.org/10.1016/j.ijadhadh.2008.07.005

McBrearty JF (1956) Fatigue and fail-safe airframe design. SAE Trans 64:426–436

Mills T, Prost-Domasky S, Honeycutt K, Brooks C (2009) Chapter 3: corrosion and threat to aircraft structural integrity. In: Corrosion control in aerospace industry. Woodhead publishing series in metals and surface engineering. 35–66. https://doi.org/10.1533/9781845695538.1.35

Milne I, Ritchie RO, Karihaloo B (2003) Interfacial and nanoscale failure, comprehensive structural integrity – section 8. Elsevier Science Ltd, Amsterdam. isbn:978-0-08-043749-1

Minford J (1981) Aluminium. 57(10):657

Mishra RS, Ma ZY (2005) Friction stir welding and processing. Mater Sci Eng R 50:1–78. https://doi.org/10.1016/j.mser.2005.07.001

Mittelstedt C, Becker W (2007) Free-edge effects in composite laminates. Appl Mech Rev 60:217–245. https://doi.org/10.1115/1.2777169

Mouritz A (2012a) Chapter 3, Materials and material requirements for aerospace structures and engines. In: Mouritz A (ed) Introduction to aerospace materials. Woodhead Publishing Limited, pp 39–56. ISBN: 978-1-85573-946-8

Mouritz A (2012b), Chapter 21, Corrosion of aerospace metals. In: Mouritz A (ed) Introduction to aerospace materials. Woodhead Publishing Limited, pp 498–520. ISBN: 978-1-85573-946-8

Mouritz A (2012c), Chapter 22, Creep of aerospace materials. In: Mouritz A (ed) Introduction to aerospace materials. Woodhead Publishing Limited, pp 521–530. ISBN: 978-1-85573-946-8

Myśliwiec P, Śliwa RE (2018) Friction stir welding of thin sheets of magnesium alloy AZ31B. Arch Metall Mater 63(1):45

Myśliwiec P, Śliwa RE, Ostrowski R (2019) Friction stir welding of ultra thin AA2024-T3 aluminium sheets using ceramic tool. Arch Metall Mater 64(4):1385–1394

Nagy PB (1991) Ultrasonic classification of imperfect interfaces. J Adhes Sci Technol 5:619–630. https://doi.org/10.1163/156856191X00521

Pawłowska P, Sliwa RE (2015) Backward extrusIon of alumInum alloy sections used in aIrcraft structural components. Arch Metall Mater 60:2805–2811

Peel CJ, Gregson PJ (1995) Design requirements for aerospace structural materials, high performance materials in aerospace. Chapman & Hall, London

Pokluda J (2010) Damage and performance assessment of protective coatings on turbine blades. Intech Eur 2010:283–304

Rebhi L, Krstic B, Boutemedjet A et al (2018) Fatigue fracture analysis of an ADF antenna in a military aircraft. Eng Fail Anal 90:476–488. https://doi.org/10.1016/j.engfailanal.2018.04.013

Rosato D (2013) Designing with plastics and composites: a handbook. Springer Science & Business Media, Boston

Rossman A (2020), Damage due to Stress Corrosion Cracking (SCC) in Aeroengine Safety, Institute of Thermal Turbomachinery and Machine Dynamics, Graz University of Technology. https://aeroenginesafety.tugraz.at/doku.php?id=5:54:542:5422:5422

Rubin AM, Jerina KL (1995) Evaluation of porosity in composite aircraft structures. Mech Compos Mater 30:587–600. https://doi.org/10.1007/BF00821276

Rupke JE (2006) What happens when lightning strikes an airplane? Scientific American, https://www.scientificamerican.com/article/what-happens-when-lightni/#:~:text=Although%20passengers%20and%20crew%20may,the%20nose%20or%20wing%20tip

Ruth AS (1973) Own work, CC by 3.0. https://commons.wikimedia.org/w/index.php?curid=25218657

Śliwa RE, Pawłowska B, Balawender T (2016) Metallic lightweight composite profiles for aviation obtained in extrusion process, AVT-264 Specialist,s Meeting on Design, Manufacturing and Application of Metallic Lightweight Material Components for Military Vehicles (NATO – unclassified + Sweden+Australia and New Zealand, NATO Conference, 2016, Tallin, Estonia

Śliwa RE, Balawender T, Hadasik E et al (2017) Metal forming of lightweight magnesium alloys for aviation applications. Arch Metall Mater 62:1559–1566. https://doi.org/10.1515/amm-2017-0239

Śliwa RE, Myśliwiec P, Ostrowski PR et al. (2019) Possibilities of joining different metallic parts of structure using friction stir welding methods. Procedia Manuf 27:158–165. https://doi.org/10.1016/j.promfg.2018.12.059

Smith T, Crane R (1980) Proceedings of the national SAMPE symposium, p 2

Sun Z, He G, Meng Q et al (2020) Corrosion mechanism investigation of TiN/Ti coating and TC4 alloy for aircraft compressor application. Chin J Aeronaut 33:1824–1835. https://doi.org/10.1016/j.cja.2019.08.015

Sweers G, Birch B, Gokcen J (2014) Lightning strikes: protection, inspection, and repair. AERO Magazine by Boeing 4:19–28

Snyder D (2014) Computational design of high-strength, SCC-resistant aluminum alloys for aerospace applications. Presented in Materials Technology Laboratory / Steel Research Group, 30th Annual Meeting, Northwestern University, 24–25 March 2014, Evanston, IL, USA. https://chimad.northwestern.edu/docs/SRG2014/SRG2014_Snyder.pdf

Thirumalaikumarasamy D, Shanmugam K, Balasubramanian V (2014) Corrosion performance of atmospheric plasma sprayed alumina coatings on AZ31B magnesium alloy under immersion environment. J Asian Ceramic Soc 2:403–415. https://doi.org/10.1016/j.jascer.2014.08.006

Thomas WM, Nicholas ED, Needham JC et al. (1991) Friction stir butt welding. International Patent Application PCT/GB92/02203 GB patent Application 9125978.8.

Tiffany CF, Gallagher JP, Babish C et al. (2010) Threats to structural safety, including a compendium of selected structural accidents/incidents, USAF Technical Report ASC-TR- 2010-5002, Aeronautical Systems Center Engineering Directorate. Wright-Patterson Air Force Base, OH 45433–7101

Tiong UH, Clark G (2010) The structural environment as a factor affecting coating failure in aircraft joints. Procedia Eng 2:1393–1401. https://doi.org/10.1016/j.proeng.2010.03.151

Tomblin J, Seneviratne W, Pillai GR (2009) Effect of disbonds, lightning strikes, and low-velocity impact damage on adhesively bonded composite joints, FAA-AR-09-4, Final Report. http://www.tc.faa.gov/its/worldpac/techrpt/ar094.pdf

Trifkovic D, Stupar S, Bosnjak S et al. (2011) Failure analysis of the combat jet aircraft rudder shaft. Eng Fail Anal 18:1998–2007. https://doi.org/10.1016/j.engfailanal.2011.05.017

Tyczyński P, Śliwa RE, Ostrowski R (2015) Analysis of possibilities for modification of drill bit geometrical parameters used to drill holes in composite materials of various composition. Aircraft Engineering and Aerospace Technology 87(2):120–130. https://doi.org/10.1108/AEAT-06-2014-0094

US National Oceanic and Atmospheric Adminstration (n.d.) Icing Tutorial, National Weather Service ZHU training page, https://www.weather.gov/source/zhu/ZHU_Training_Page/ZHU_Training_Page.html

Vanclooster K, Lomov SV, Verpoest I (2009) On the formability of multi-layered fabric composites. in ICCM—17th International Conference on Composite Materials. Edinburgh, United Kingdom

Vijayan S, Raju R (2008) Process parameter optimization and characterization of friction stir welding of aluminum alloys, International Journal of Applied Engineering Research, 3:1303–1316

Vorontsov AN, Murzakhanov GK, Shchugorev VN (1990) Delamination failure of composite structures. Mech Compos Mater 25:723–737. https://doi.org/10.1007/BF00613361

Wanhill RJH, Amsterdam E (2010) Aircraft Stress Corrosion in the Netherlands: 1965–2010, National Aerospace Laboratory (NRL) Report.

Wen Q, Li WY, Wang WB et al (2019) Experimental and numerical investigations of bonding interface behavior in stationary shoulder friction stir lap welding. J Mater Sci Technol 35:192–200. https://doi.org/10.1016/j.jmst.2018.09.028

Wisnom MR (1993) Analysis of shear instability in compression due to fibre waviness. J Reinf Plast Compos 12:1171–1189. https://doi.org/10.1177/073168449301201103

Xu S, Deng X, Reynolds AP et al. (2001) Finite element simulation of material flow in friction stir welding. Sci Technol Weld Joining 6:191–193. https://doi.org/10.1179/136217101101538640

Zhang YN, Cao X, Larose S et al (2012) Review of tools for friction stir welding and processing. Can Metall Q 51:250–261. https://doi.org/10.1179/1879139512Y.0000000015

Zhou JM, Lucas JP (1995) The effects of a water environment on anomalous absorption behaviour in graphite-epoxy composites. Compos Sci Technol 53:57–64. https://doi.org/10.1016/0266-3538(94)00078-6

Zhou JM, Lucas JP (1999a) Hygrothermal effects of epoxy resin. Part I: the nature of water in epoxy. Polymer 40:5505–5512. https://doi.org/10.1016/S0032-3861(98)00790-3

Zhou JM, Lucas JP (1999b) Hygrothermal effects of epoxy resin. Part II: variations of glass transition temperature. Polymer 40:5513–5522. https://doi.org/10.1016/S0032-3861(98)00791-5